Characterization of the metabolic properties of brain microvascular endothelial cells

By

Nicholas A. Marinelli

Thesis

Submitted to the Faculty of the Graduate

School of Vanderbilt University in partial

Fulfillment of the requirements for the

degree of

Master of Science

In

Chemical and Physical Biology

August 9, 2019

Nashville, Tennessee

Approved:

Ethan S. Lippmann, Ph.D.

Vivian Gama, Ph.D.

Bruce M. Damon, Ph.D.

ACKNOWLEDGEMENTS

This work would not have been possible without the gracious financial support from the Integrated Training in Diabetes and Engineering NIH T32 Training grant. I am especially grateful for the support from Dr. Ethan Lippmann over the course of my work, who has worked with me to develop and complete a project to help me fulfill my career goals. Dr. Lippmann has helped me become a better scientist, colleague, and person. I had the opportunity to work with incredible people both within the lab, and through collaboration with other groups and I could not have asked for a better place to have spent my time while at Vanderbilt.

TABLE OF CONTENTS

LIST OF TABLES

LIST OF FIGURES

Chapter 1: Introduction

1.1. The Blood-Brain Barrier Overview

The blood-brain barrier (BBB) is a highly restrictive and regulated vascular network, strictly controlling the molecules that enter the brain via the bloodstream, while also serving an important role in removing toxic compounds from the brain. Brain microvascular endothelial cells (BMECs) form the BBB by lining capillaries and separating the bloodstream from the brain[1]. The physiological barrier provided by these cells is coordinated by a combination of unique properties possessed by the BMECs. These specialized endothelial cells prevent paracellular diffusion of ions and hydrophilic molecules via high-fidelity intercellular tight junctions, suppress nonspecific pinocytosis/transcytosis activity[2-3], employ a variety of solute carriers to shuttle biomolecules to and from the brain[4], and express a variety of efflux transport proteins that prevent small, lipophilic compounds from passively diffusing through the BMEC lipid bilayer[5]. Thus, the BBB provides control over the extracellular milieu in neural tissue, a feature that permits proper neuronal function, which requires precise ionic concentration in the surrounding environment[6]. The BMEC-forming BBB interacts with other cell types in the central nervous system (CNS), including neurons, astrocytes, pericytes, and microglia, to form the neurovascular unit (NVU). The NVU protects the CNS from injury via the entry of toxins, pathogens, and the body's own immune response[7], and its disruption is a crucial event in many cerebrovascular and neurodegenerative disorders, including Alzheimer's disease and Parkinson's disease. As such, a better understanding of the mechanisms regulating the BBB during health and disease is expected to provide potentially groundbreaking insights for treatment of a variety of neurological disorders[8].

1.2. Modeling of the Blood-Brain Barrier *in vitro*

Early attempts to model the BBB utilized non-CNS endothelial cells such as human umbilical vein endothelial cells (HUVECs)[9]. HUVECs, derived from the endothelium of umbilical cord veins shortly after childbirth rather than a cerebral origin, express some of the junction and transport proteins found in BMECs, but do not form the tight barrier characteristic of the BBB[10]. An important step forward was the successful isolation of brain capillaries from both human and animal sources, which was subsequently followed by

preliminary brain endothelial cell cultures[11]. However, there are significant limitations to these sources. First, human BMECs are extremely limited and difficult to obtain[12]. While cells isolated from rodent sources help to overcome the limited availability of human cells, many rats and/or mice are needed to obtain enough cells for experimental purposes[13]. Although pigs and cows can provide significantly more cells than rodents, access to these animals is more difficult, and the biochemical and molecular characteristics are not as well characterized[14].

Given the limitations of primary cells (*e.g*. high cost and special skills required for isolation), several immortalized cell lines were developed from isolated animal cells that could be used for many passages and still maintain some of their BBB characteristics. Two widely used cell lines are the rat brain endothelial cell line RBE4 and the mouse brain endothelial cell line b.End3-5[15]. These cell lines were widely used to study transporter properties, as they retained functional expression of p-glycoprotein. They were also used to study signaling pathways and for BBB permeability studies[16]. However, despite being the best available option for many years, they are still of non-human origin and thus differ significantly from human BMECs. The advent of immortalized human brain endothelial cells led to more accurate studies of the BBB. Specifically, the hCMEC/D3 cell line retains expression of some tight junction proteins and active efflux transporters, making a widely used model to study drug transport across the BBB[17-18]. However, hCMEC/D3 cells lack appreciable are paracellular barrier function, and therefore are not suitable for permeability studies. As such, a BBB model that could more accurately recapitulate *in vivo* properties represented a significant need in the field.

In 2012, human pluripotent stem cells (hPSCs) were successfully differentiated to BMECs, as determined by increased transendothelial electrical resistance (TEER) (~850 Ω x cm^2), representative permeability to a cohort of small molecules, and active efflux transporter function[19]. TEER is a measure of passive barrier function that arises from the tight junction protein interactions between adjacent BMECs. The addition of retinoic acid (RA) during the differentiation process further enhanced passive barrier function (TEER ~3,000 Ω x cm^2)[20]. The use of hPSC-derived BMECs has greatly enhanced studies of the BBB, as they are a theoretically limitless source while maintaining many of the properties observed *in vivo*[23]. These BMECs have are effective for modeling BBB-specific disease mechanisms[22] and have been used for mechanistic interrogations[21], including precise metabolic studies of the BBB.

1.3. Cellular Metabolism

From a fundamental biology perspective, all organisms must convert nutrients into energy, and cells utilize one of two pathways to meet their energetic demands: glycolysis or oxidative phosphorylation[24]. Glycolysis occurs in the cytoplasm and breaks glucose down to pyruvate, which can then be enzymatically converted to lactate via lactate dehydrogenase. This process produces adenosine triphosphate (ATP), the cell's primary energy source[25-28]. Typically, a cell will only convert pyruvate to lactate in anaerobic conditions in order to regenerate cofactors that are necessary for upstream reactions in glycolysis. Alternatively, cells can utilize oxidative phosphorylation by carrying out a series of redox reactions that involves the oxidation of glucose (following glycolytic breakdown to pyruvate), amino acids, and other macromolecules. Oxidative phosphorylation occurs in the cell's mitochondria and is much more efficient at generating ATP than glycolysis; however, it requires abundant oxygen[29-32]. Intriguingly, peripheral endothelial cells (ECs) are generally highly glycolytic in their use of glucose, despite their close proximity to oxygen rich blood[11]. This phenomenon, known as the Warburg Effect, was originally observed in cancer cells that were hyperglycolytic even while residing in aerobic environments[29-32]. Peripheral ECs have low mitochondrial volume fractions and their mitochondria are generally viewed as "signaling hubs" rather than "metabolic powerhouses."[33-35] However, BMECs have significantly higher mitochondrial fractions (>5-fold relative to muscle capillaries)[36], and whereas peripheral vasculature is much more plastic, turnover rates in mature healthy BMECs are on the order of years, which indicates a more quiescent and non-proliferative state that may rely on different metabolic pathways. Finally, many of the functions that give the BBB its restrictive properties (e.g. transporter activity) are ATP-dependent, suggesting an increased role for oxidative phosphorylation. Collectively, these findings indicate, that relative to peripheral ECs, BMECs may utilize unique metabolic functions that underlie their specialized properties.

Chapter 2: A Fully Defined Differentiation Scheme for Producing BMECs from Human Induced Pluripotent Stem Cells (iPSCs)

2.1. Introduction

The initial differentiation of hPSCs to BMECs, as well as the RA enhanced differentiation scheme, opened the door for robust and accurate studies of the human BBB. However, there were still limitations in the differentiation process. TEER has been estimated *in vivo* up to 8,000 Ω x cm^2 based on radioactive ion permeabilities[37], and although this value may not be the absolute upper limit in humans, hPSC-derived BMECs in monoculture typically exhibit about half of this TEER threshold[38-39]. Moreover, BMEC differentiation relies on the use of serum-containing medium, which limits consistency and reliability of the final purified cell population. Despite advancements in standardization of the differentiation process[39-40], more work is needed to achieve optimum results. As such, we identified an improvement to the BBB differentiation process while transitioning to serum-free methods. In addition to enhancing overall efficiency, moving to fully defined conditions in the BMEC differentiation scheme will enhance and facilitate metabolic studies. Serum is undefined, so the nutrient composition available to the cells cannot be controlled. This limits metabolic studies because it is difficult to account for the confounded influence of serum in nutrient consumption and metabolite production. By replacing the serum component of the differentiation medium with fully defined factors, we can consistently achieve TEER maxima of 2,000-8,000 Ω x cm^2 in BMEC monocultures across multiple iPSC lines, with expected marker expression and transporter activity. Moreover, the exclusion of serum significantly enhanced the responsiveness of BMECs to co-culture with astrocytes, with maximum TEER values reproducibly exceeding 9,000-10,500 Ω x cm^2. These advances in differentiation technique are expected to have a positive impact toward using iPSC-derived BMECs to model age- and disease-related declines in BBB function in addition to mechanistic studies of the metabolic regulation of the BBB.

2.2. Experimental Design

2.2a. iPSC differentiation to BMECs

iPSCs are maintained in E8 medium[41], prepared in-house as previously described[39], on growth factor reduced Matrigel. When iPSCs were 60-80% confluent, the cells were washed once in DPBS and incubated in Accutase for 3-5 minutes at 37°C. The resultant single cell suspension was collected via centrifugation, resuspended in fresh E8 medium containing 10 μM of the ROCK inhibitor Y-27632. Cells were counted using Trypan blue cell viability assay and seeded at a density of ~15,000 cells/cm^2. 24 hours after seeding, medium was changed to E6 medium[42] to induce differentiation. Medium was changed daily for 4 days. Next, cells were given human endothelial serum free medium (hESFM) supplemented with 20 ng/mL bFGF, 10 μM RA, and either platelet-poor plasma-derived serum (PDS) or a serum-free supplement (B27, N2, or insulin, transferrin, and selenium [ITS]). Medium was not changed for 48 hours. After 48 hours, cells were washed once with DPBS and incubated with Accutase for 20 minutes to 45 minutes, until a single cell suspension was formed. Cells were collected via centrifugation and plated onto substrates coated in a mixture of 400 μg/mL collagen IV and 100 μg/mL fibronectin. Substrates were either tissue culture polystyrene plates or Transwell filters with 1.1 cm^2 polyethylene terephthalate membranes with 0.4 μm pores. This process of replating, also referred to as subculturing, is a purification step to remove any neural precursor cells generated during the differentiation and to obtain a pure BMEC population. Cells were replated using a ratio of 1 well of a 6-well plate to 3 wells of a 12-well plate, 3 Transwell filters, or 6 wells of a 24-well plate. Media was then changed 24 hours later to the basal endothelial cell media with desired supplement, but lacking bFGF and RA. TEER was measured 24 hours after subculturing, and approximately every 24 hours for the duration of the experiment.

2.2b. TEER measurement

All TEER plots presented are the results of N=1 biological sample. Each time point is a result of a technical N=9 as BMECs were purified onto triplicate filters for all conditions tested, and each filter was measured in 3 locations per time point. All data are represented as mean ± standard deviation for these collective measurements. All results were confirmed in a minimum of two biological replicates. Following the

medium change on day 0 of subculture to remove bFGF and RA, no further medium changes were performed for the duration of the experiments. TEER was measured using STX2 chopstick electrodes and an EVOM2 voltohmeter.

2.2c. Immunocytochemistry

Cells were washed twice with DPBS and incubated in either 4% paraformaldehyde (PFA) for 20 minutes or 100% ice-cold methanol for 10 minutes. Cells were then washed three times in DPBS for a minimum of 5 minutes per wash. Cells fixed in 4% PFA were pre-blocked for a minimum of 1 hour at room temperature in DPBS with 5% donkey serum and 0.3% Triton X-100, referred to as PBS-DT. Cells fixed in methanol were pre-blocked for a minimum of 1 hour at room temperature in DPBS with 5% donkey serum, referred to as PBSD. Cells were then incubated with the respective primary antibodies at the desired dilution in either PBS-DT or PBSD overnight at 4°C. Cells were rinsed once with DPBS, then washed 5 times for a minimum of 5 minutes per wash using DPBS. Secondary antibodies were diluted 1:200 in PBS-DT or PBSD and incubated for 1-2 hours at room temperature. Following this incubation, nuclei were labeled using 4',6-Diamidino-2-phenyl-lindoldihydrochloride (DAPI) or Hoechst 33342 trihydrochloride trihydrate diluted in DPBS for 10 minute. DAPI or Hoechst was then removed, cells rinsed once in DPBS, and then washed 5 times with DPBS for a minimum of 5 minutes per wash. Cells were visualized on a Leica DMi8 microscope.

2.2d. Sodium fluorescein permeability assay

BMECs subcultured onto Transwell filters were given fresh medium (hESFM with one of the respective supplements) 1 hour prior to the start of the assay. Medium was then aspirated from the apical chamber only and replaced with 10 μM sodium fluorescein diluted in fresh medium. 200 μL of medium was immediately removed from the basolateral chamber of each filter, transferred to a 96-well plate, and replaced with 200 μL fresh medium. This process was repeated every 30 minutes (x 5) for a total of 2 hours. This was also conducted concurrently on Transwell filters coated with collagen/fibronectin solution but lacking cells. Fluorescence of the collected samples was measured using a BioTek Synergy H1 multi-mode plate reader. The effective permeability (P_e) was calculated as previously described[21]. This was performed for a biological

N=3, and for each replicate, the flux of sodium fluorescein across cell monolayers was measured using 3 Transwell filters as well as one control filter coated with collagen and fibronectin but lacking cells. Transport across a Transwell filter lacking cells was also used measured to correct permeability values for mass transfer resistance due to the filter.

2.2e. Efflux transporter activity assay—Substrate accumulation

iPSCs were subcultured onto 24-well plates and treated with endothelial medium lacking bFGF and RA for 24 hours prior to the assay. For inhibitor conditions, BMECs were incubated with 10 μM cyclosporine A (CsA) or 10 μM MK571 for 1 hour at 37°C. After this incubation, cells were incubated with 10 μM rhodamine 123 (R123) or 10 μM 2',7'-dichlorodyhydrofluorescein diacetate (H_2DCFDA) with or without their respective inhibitors for 1 hour at 37°C. Following this second incubation, 3 wells per condition were washed twice with DPBS and lysed using DPBS containing 5% Triton X-100. The remaining well of cells per each condition was fixed using 100% ice-cold methanol. The fluorescence of the lysed wells was measured using a BioTek Synergy H1 multi-mode plate reader and the fixed cells were incubated with DAPI for 10 minutes. Each well of the fixed cells was imaged in 6 locations and nuclei were counted using Fiji[43], and fluorescence values were normalized on a per-cell basis. All conditions were performed using triplicate wells to calculate mean ± standard deviation. Reported trends were confirmed across two additional biological replicates.

2.2f. Efflux transporter activity assay—Directional Transport

BMECs on Transwell filters were incubated with 10 μM CsA or MK571 diluted only in the apical chamber for 1 hour at 37°C. Next, BMECs were incubated with 10 μM R123 or H_2DCFDA with or without CsA or MK571, respectively, for 1 hour at 37°C. At the end of the incubation, 200 μL of medium was removed from the basolateral chamber of each filter and fluorescence was measured using a plate reader. Fluorescence values were normalized to medium collected from the basolateral chamber of BMECs not treated with inhibitor. The assay was performed using triplicate filters, and reported values were calculated as mean ± standard deviation. Reported trends were confirmed across two additional biological replicates.

2.2g. Statistical analyses

All data are expressed as mean ± standard deviation. Student's unpaired t-test was used to determine statistical significance for all efflux transport accumulation and directional transport assays. Statistical significance was verified across all biological replicates, where a minimum of three independent experiments was performed.

2.3. Results

2.3a. Serum-free medium yields iPSC-derived BMECs with enhanced TEER

The influence of serum and serum-derived proteins on hPSC differentiation has been well-documented[61], and the development of fully defined differentiation protocols is thus recognized as an important step for standardizing hPSC research applications. Importantly, a fully defined protocol will open the door to metabolic studies of the BBB and provide novel routes of mechanistic interrogation. Accordingly, we sought to replace the serum in our BBB differentiation process with more defined components. Our current differentiation scheme uses PDS as a supplement in the basal medium on day 4, and again when BMECs are purified on day 6 (**Figure 1A)**. The influence that PDS has on the differentiation is strikingly observed when comparing passive barrier properties of BMECs derived from two different lots of PDS (**Figure 1B)**. Indeed, 44% of BMEC differentiations fail to reach TEER exceeding 1,000 Ω x cm^2 using a single lot of PDS, while differentiations conducted using a second lot of PDS consistently reached TEER maxima in excess of 2,000 Ω x cm^2. When we replaced PDS with B27, a common serum alternative in neural cultures, tested at either the manufacturers recommendation (50X dilution) or 200X dilution, B27 supplementations produced maximum TEER above 8,000 Ω x cm^2 (8,734 ± 349 Ω x cm^2 in 200X B27) (**Figure 1C**). CC3-derived BMECs and CD10-derived BMECS, female and male control lines[44-45], respectively, consistently achieved maximum TEER values in excess of 3,000 Ω x cm^2 across more than 10 independent CC3 differentiations and in excess of 2,000 Ω x cm^2 across 4 independent CD10 differentiations (**Figure 1D-E**).

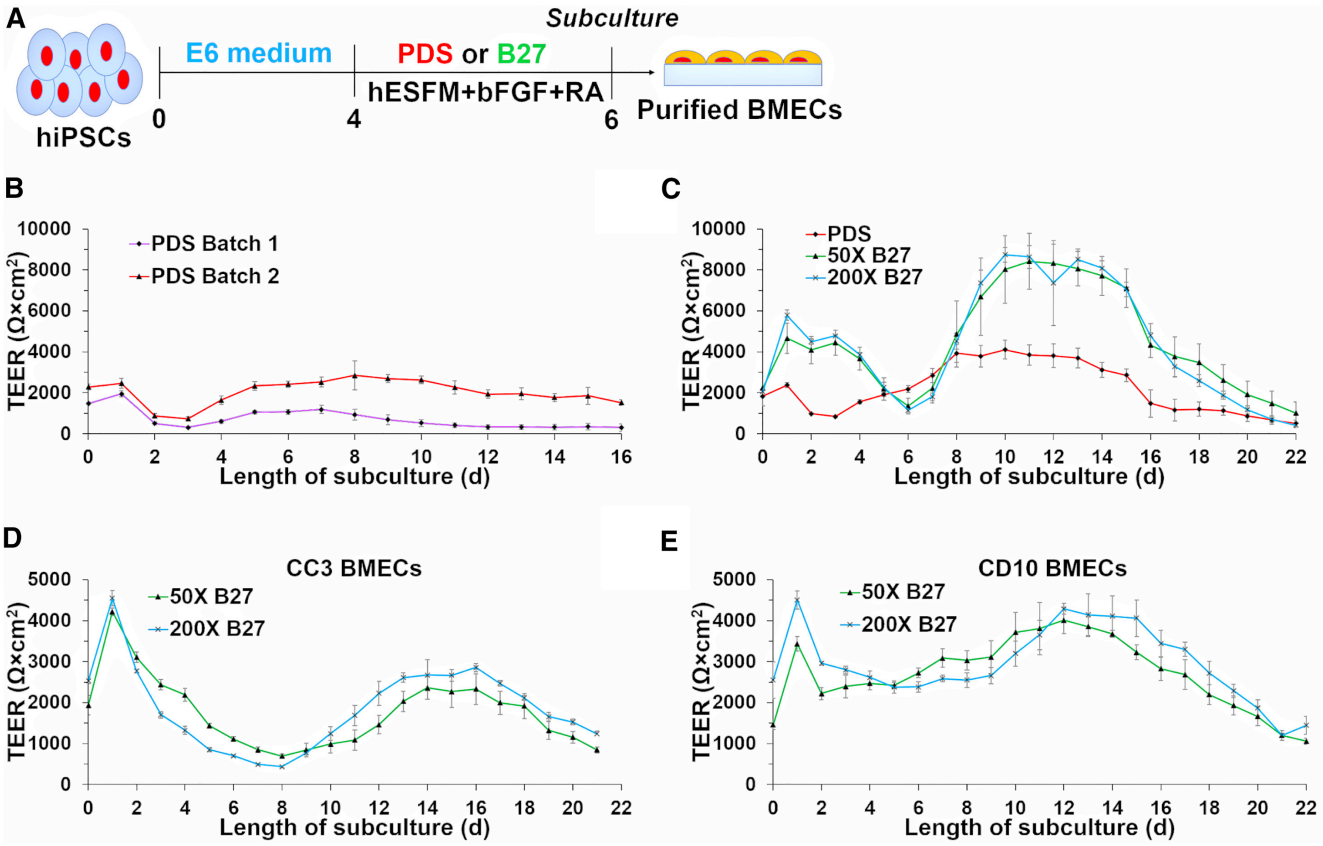

Figure 1: Replacing serum with B27 during BMEC differentiation increases consistency. A) Timeline of differentiation with altered media composition (PDS vs B27). B) PDS batch-to-batch variability demonstrated by the significant differences in TEER between two separate batches. C) Replacing PDS with B27 increases TEER at multiple dilutions D) and E) CC3 (female) and CD10 (male) iPSC-derived BMECs both exhibit higher TEER across N = 3 biological replicates.

2.3b. Additional characterization of iPSC-derived BMEC phenotype under serum-free conditions

In addition to TEER measurements, we assayed other properties of iPSC-derived BMECs under serum-free conditions. Before purification (day 6), BMECs expressed occludin, claudin-5, VE-cadherin, GLUT-1, and PECAM-1, indicating both acquisition of BBB phenotype and endothelial cell identity as typically seen in PDS (**Figure 2A**), and BMECs maintained expression of these markers 48 hours after purification (**Figure 2B**). Furthermore, paracellular permeability was assessed using sodium fluorescein, and all replicates had effective permeability's less than 2.5 x 10^{-7} cm/s, similar to BMECs differentiated in PDS[39] (**Figure 2C**). Collectively, these results indicate that replacement of serum with B27 during differentiation produces BMECs with robust

passive barrier properties, while eliminating the reliance on an undefined material with substantial lot-to-lot variability. Next, we evaluated efflux activity of P-glycoprotein (PGP) and multidrug resistance protein (MRP) transporters. PGP activity was assessed by measuring fluorescence accumulation after BMECs were incubated with either R123, a PGP substrate, or R123 containing CsA, a PGP inhibitor. BMECs incubated with the inhibitor showed a significant increase in fluorescence accumulation, indicating active PGP function (**Figure 2D**). Similarly, purified BMECs were incubated with H_2DCFDA with or without MK571, an inhibitor of the MRP family, and showed increased fluorescence accumulation compared to control cells, indicating MRP activity (Figure 2D). We then assessed directionality of PGP and MRP by measuring the transport of the fluorescent substrate across the monolayer of purified BMECs cultured on Transwell filters. Increased apical-to-basolateral substrate transport (mimicking blood-to-brain) was observed on BMECs treated with CsA and MK571 (**Figure 2E**), indicating the expected PGP and MRP polarization. Last, we co-cultured BMECs with astrocytes, an important component of the NVU and re-evaluated TEER. The BMECs co-cultured with astrocytes reach higher TEER by day 11 of subculture compared to BMECs in monoculture, exceeding 9,000 Ω x cm^2 in biological replicates (**Figure 2F**). These results indicate that BMECs are responding to astrocytic cues, a key characteristic of the BBB and NVU when functioning properly.

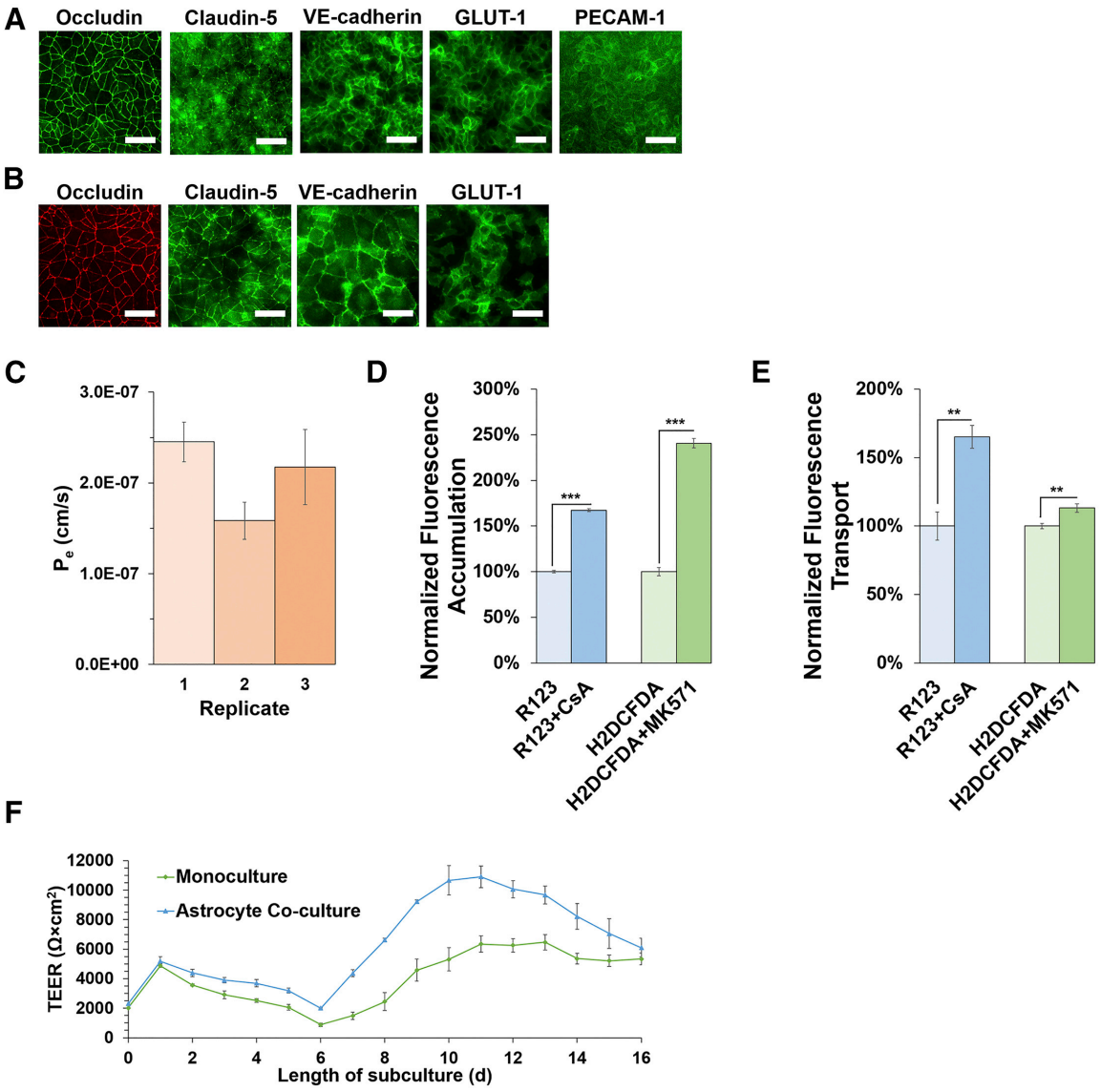

Figure 2. Full characterization of barrier properties when differentiated with B27. A) Immunostaining confirms BMECs are positive for occludin, claudin-5, VE-cadherin, GLUT-1, and PECAM-1 on day 6 of differentiation. B) Immunostaining confirms BMECs are positive for occluding, claudin-5, VE-cadherin, and GLUT-1 48 hours after purification. C) Effective permeability to sodium fluorescein when BMECs are differentiated with B27. D) Intracellular fluorescence accumulation measured when cells are incubated with PGP and MRP substrates and inhibitors. E) Apical to basolateral flux of R123 and H_2DCFDA in the presence and absence of CsA and MK571, respectively. F) TEER plot of CC3 derived BMECs co-cultured with CC3 derived astrocytes.

2.3c. Fully defined medium with minimal components can produce high-fidelity BMECs

We sought to identify specific components of B27 that were essential to a successful BMEC differentiation in order to further simplify the differentiation scheme. To this end, iPSCs were differentiated using N2, a chemically defined, serum-free replacement with known component concentrations[46], in place of B27. BMECs differentiated in N2 consistently achieved TEER values greater than 2,500 Ω x cm^2 across seven biological replicates, indicating the presence of an intact endothelial monolayer and suggesting a successful differentiation (**Figure 3A**). We further noted that insulin, transferrin, and selenium were among the conserved components between N2 and B27, and are also core components of E6 medium. Thus, we postulated that basal endothelial medium supplemented with insulin, transferrin, and selenium (referred to as ITS) might be suitable for BMEC derivation. Indeed, the resultant BMEC monolayers achieved TEER values greater than 2,500 Ω x cm^2 across seven biological replicates **(Figure 3A)**. Additionally, the long-term stability on CC3-derived BMECs was tracked and found to be similar to that of BMECs differentiated in B27 and N2 (**Figure 3B**). The use of ITS was validated in CD10-derived BMECs, as long term TEER was similar to CC3-derived BMECs (**Figure 3C**). Importantly, BMECs differentiated via the ITS scheme uniformly express VE-cadherin, occludin, claudin-5, and GLUT-1 (**Figure 3D**). Moreover, cells differentiated in ITS displayed restrictive permeability to sodium fluorescein (**Figure 3E**) and active PGP and MRP function (**Figure 3F**), indicating acquisition of BMEC phenotype. Thus, the undefined, serum-based differentiation procedure used to previously produce BMECs from iPSCs can ultimately be reduced to three fully defined media additives without compromising passive barrier integrity.

A

Cell Line	Supplement	Maximum TEER (Ω×cm²)	
CC3	N2	4379 ± 469	4310 ± 202
		3994 ± 243	3505 ± 114
		4056 ± 43	3133 ± 97
		2714 ± 78	
	ITS	5145 ± 173	2597 ± 108
		3354 ± 122	2671 ± 285
		3869 ± 164	3177 ± 127
		3985 ± 769	

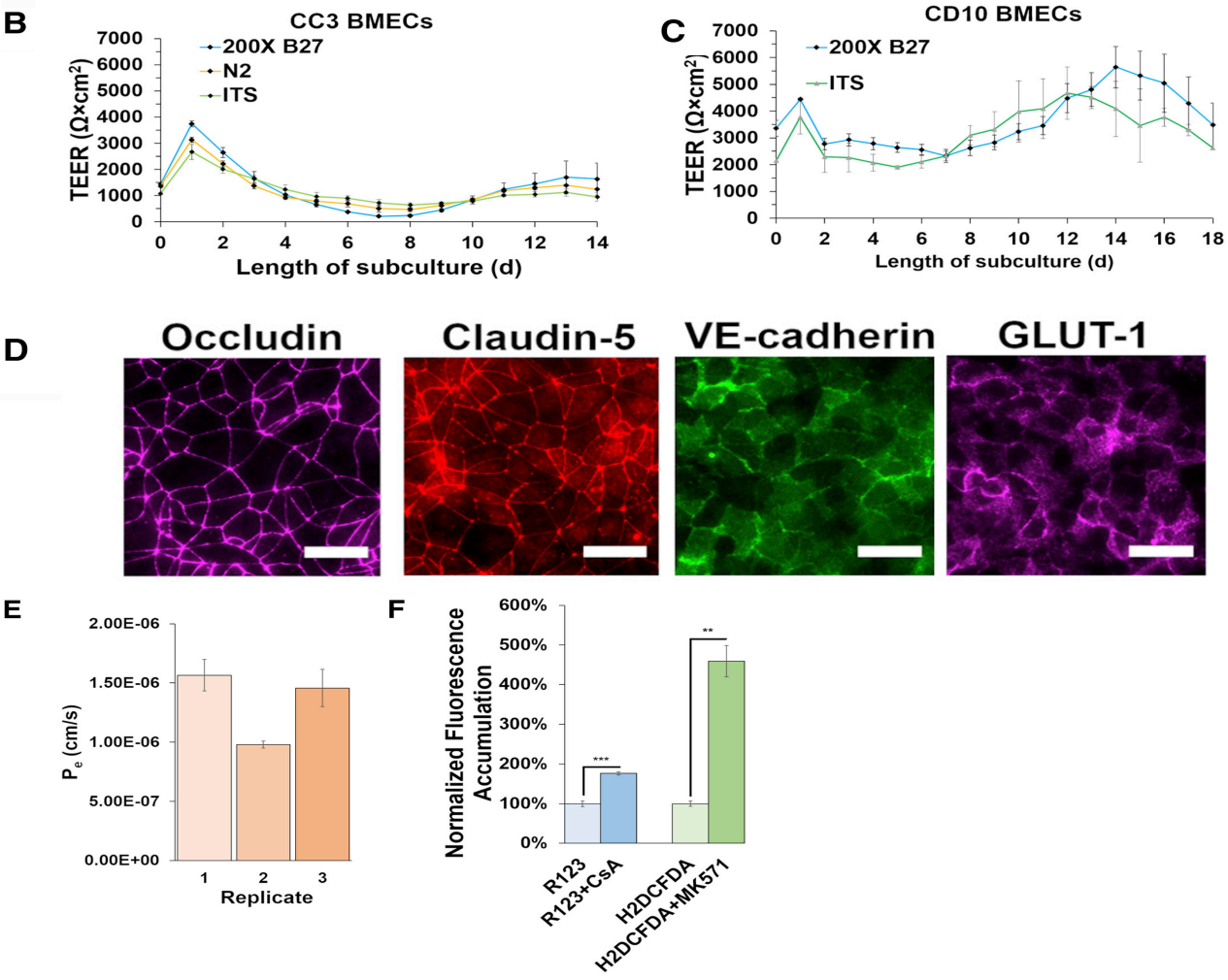

Figure 3: B27 can be simplified further to a fully defined supplement consisting of as few as 3 components. A) Maximum TEER values from 7 biological replicates when CC3-iPSCs were differentiated to BMECs using N2 or a cocktail of insulin, selenium, and transferrin (ITS). B-C) TEER plots show long term stability of CC3 and CD10-derived BMECs using N2 (CC3 only) and ITS compared to 200X B27. D) Immunostaining confirms BMECs are positive for occludin, claudin-5, VE-cadherin, and GLUT-1 hours after purification in CC3 BMECs. E) Effective permeability of sodium fluorescein for CC3-derived BMECs using ITS. F) Intracellular fluorescence accumulation was measured in CC3-derived BMECs using ITS incubated with PGP and MRP substrates and inhibitors.

2.4. Discussion

The variability of differentiation outcomes resulting from batch-to-batch changes in serum composition and quality represents a significant hurtle in the use of iPSCs for research and prospective regenerative medicine applications. This work sought to address this issue in the context of BMEC differentiation through the replacement of serum with more defined supplements. Ultimately, this advancement mitigates procedural variability, thereby providing researchers with more reliable and robust iPSC-derived BMECs to interrogate neurovascular function. Importantly, the use of a fully defined differentiation schematic permits precise and accurate metabolic studies that are not attainable when using serum. Although a recent publication demonstrated a fully defined differentiation procedure in which iPSCs were differentiated to BMECs as a homogenous population through a mesoderm intermediate, all previous BMEC differentiation procedures have relied on a co-differentiation approach in which the resultant BMECs must be purified from the mixed neural/endothelial cultures. Despite the differences in approaches, we suspected that the use of fully defined components may translate to the co-differentiation system used by most researchers. Indeed, BMECs differentiated using B27 yielded a maximum TEER that exceeded 8,000 Ω x cm^2 in monoculture, and consistently produced BMECs that with elevated TEER across multiple cell lines compared to BMECs differentiated with PDS. We note that every differentiation did not produce BMECs with TEER up to the *in vivo* levels, nor did the CD10 male-control line. We speculate that these differences may be due to subtle differences in culture technique between users and metabolic and passage differences between iPSC lines.

Finally, despite the advantages of B27 as a serum-free supplement, we were concerned that its composition is proprietary and not completely defined, as it contains albumin. BBB function can be influenced by different components that regulate diverse signaling pathways[47]; therefore, if the goal of the experiment is to dynamically investigate the influence of any one particular component on BBB function in real-time, it is desirable to precisely control composition of the medium. As such, we evaluated a chemically defined supplement (N2), as well as a defined mixture of insulin, transferrin, and selenium. Remarkably, regardless of the composition, the resultant BMECs achieved passive barrier properties well above those considered to be a function barrier (TEER above 500-1000 Ω x cm^2)[48] These BMECs also displayed active PGP and MRP function. Overall, the use of fully defined medium represents a robust, reproducible, and cost-effective

approach to investigating BBB physiology *in vitro*, thereby facilitating broader adoption of iPSC-derived BMEC models across the greater research community. Importantly, this work sets the stage for future metabolic studies aimed at identifying underlying mechanisms regulating tissue barrier function.

Chapter 3: Basal Media Influences Barrier Formation and Maintenance

3.1. Introduction

The basal medium in all published iPSC-derived BMEC studies is human endothelial serum-free medium (hESFM), and until our recent work, has utilized serum during the differentiation process. While replacing serum with fully defined components represents a significant step to reproducibly differentiate iPSCs to high-fidelity BMECs, limitations still exist. Particularly, the composition of hESFM is proprietary, making it difficult to ascertain the role that individual components may have on barrier formation and maintenance. Furthermore, to precisely interrogate potential drug targets, metabolic pathways, and other underlying molecular mechanisms regulating tissue barrier function, a medium with known compositions that is also suitable to customization is highly desired. To this end, we explored the responsiveness of human BMECs to biomolecule availability using basal media with known compositions. As such, Neurobasal medium (NB medium), originally developed to maintain neural cultures, and Dulbecco's Modified Eagle Medium/F-12 (DMEM/F12, referred to hereafter as DMEM), which is used for a variety of cell applications, are both readily available with published compositions. The use of NB medium during differentiation and purification yielded robust barrier formation equal to hESFM, with a TEER of 5,000-7,000 $\Omega \times cm^2$. Surprisingly, the use of DMEM yielded BMECs with a significantly lower barrier function (TEER ~1,000 $\Omega \times cm^2$). Importantly, DMEM and NB medium are highly similar in composition, differing mainly by slight differences in amino acid composition and vitamin composition. Therefore, the experiments carried out in this work are critical to the identification of components required for BMECs to form and maintain a tight barrier. Finally, these results will enhance our understanding of how metabolism may contribute to loss of barrier function in the context of neurodegenerative disease.

3.2. Experimental Design

3.3a. iPSC differentiation to BMECs and assays characterizing baseline BMEC function

The iPSC-to-BMEC differentiation schematic, TEER measurements, immunocytochemistry, sodium fluorescein assays, and efflux transporter assays were carried out as described in section 2.2 with the notable difference that hESFM was replaced with DMEM or NB medium during differentiation **(Figure 4A)**. Additionally, functional assays were performed at different time points than outlined above, and each scenario is outlined below and later in section 3.3.

On day 4 of differentiation, iPSCs were switched to DMEM or NB medium supplemented with B27, 20 ng/mL bFGF, and 10 μM RA. BMECs were subcultured on day 6 in the same media they were differentiated in (i.e. if BMECs were differentiated in NB medium, they were then subcultured in NB, and vice versa with DMEM). Media was changed 24 hours after subculture to the respective basal medium used during differentiation, lacking bFGF and RA. TEER was measured every 24 hours for the duration of the experiment.

To determine if the differential TEER results were due to intrinsic developmental differences during differentiation, medium was changed a second time at various time points. In this case, BMECs differentiated in NB medium were subcultured and matured in NB medium, then subsequently changed to DMEM or replaced with NB medium to control for any effect that fresh medium may have on the barrier function. Medium was changed for the second time at either 48 hours or 7 days post-subculture, and TEER was measured until the cells lost barrier fidelity (i.e. TEER dropped below ~1,000 Ω x cm^2).

We then went on to characterize barrier active and passive barrier properties via sodium fluorescein permeability assays and efflux transporter assays. Sodium fluorescein assays were performed as previously described with the following modification. Instead of performing the assay 24 hours after removing bFGF and RA, the assay was performed 48 hours after removal of these factors to correspond to the second change in media outlined above.

3.3. Results

3.3a. Basal media effects TEER in mature iPSC-derived BMECs

The basal medium in all published iPSC-derived BMEC work has been hESFM, a proprietary mixture. Despite significant advances from our group to remove serum from the differentiation process and to develop a fully defined differentiation scheme, limitations remain when studying specific underlying mechanisms involved in barrier regulation. Because the components of hESFM are unknown, it is impossible to discern what exactly affects change on the barrier. As such, we sought to use medium with published components that would be suitable for customization and manipulation. The use of NB medium in place of hESFM during differentiation and purification resulted in robust barrier formation equal to hESFM, with TEER ~5,000-7,000 Ω x cm^2 (**Figure 4B)**. Intriguingly, the use of DMEM yielded BMECs with significantly lower barrier function, with TEER ~1,000-2,000 Ω x cm^2 (**Figure 4B)**. Furthermore, a 50/50 mixture of the two compositions yielded slightly better TEER, but not a substantial recovery (**Figure 4B)**. Importantly, these effects were not due to improper endothelial cell differentiation, as they uniformly expressed VE-cadherin and maintained smooth occludin$^+$ tight junctions **(Figure 4C)**.

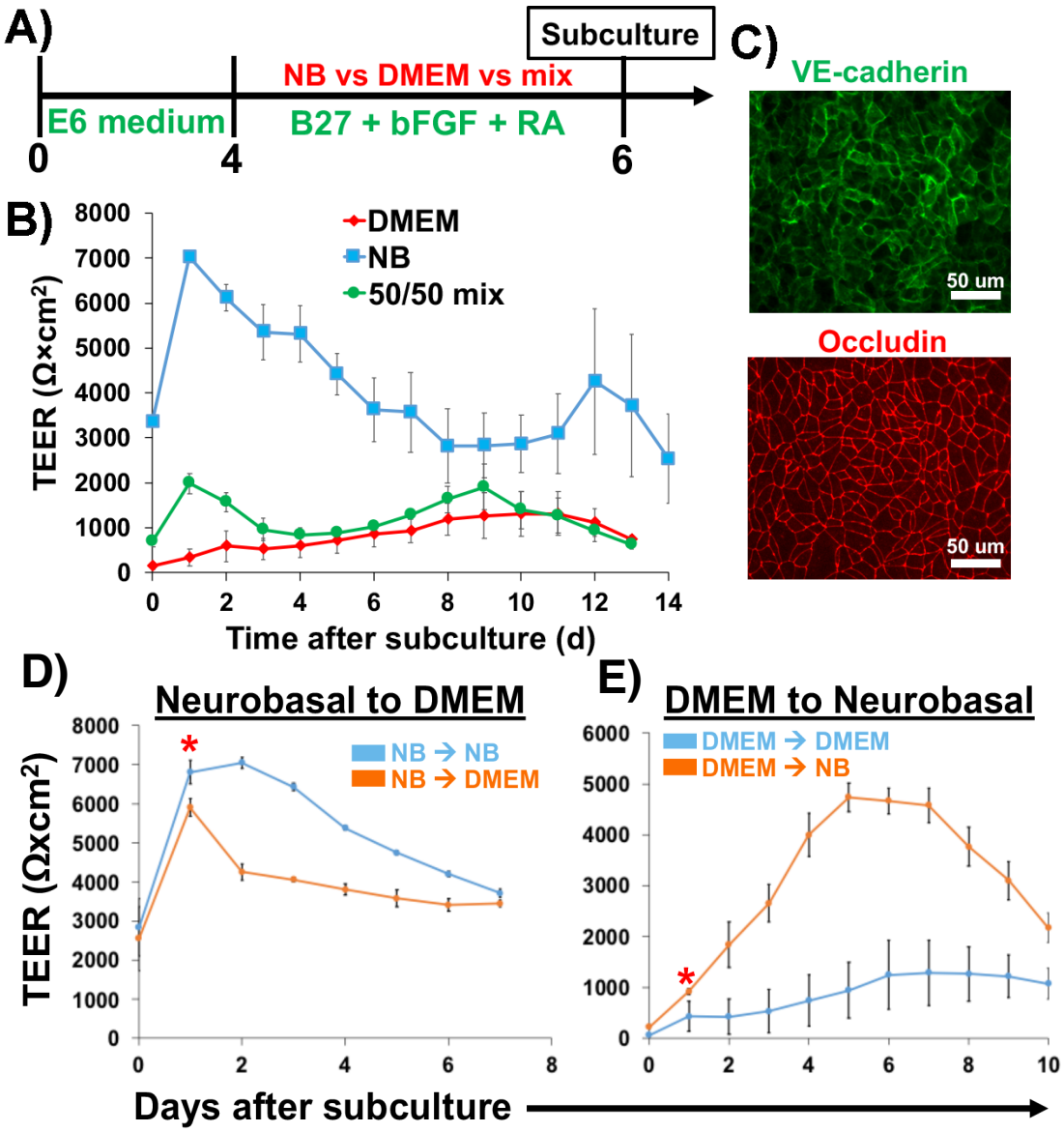

Figure 4. Influence of basal media on BBB properties. A) Timeline of differentiation with altered media composition. B) TEER plots for iPSC-derived BMECs in monoculture with different basal media. Biological N = 3 was used to confirm observed trends. C) Immunostaining was used to confirm that iPSCs differentiated in DMEM still form VE-cadherin+/occludin+ endothelial cells despite reduced barrier properties. D-E) iPSC-derived BMECs were either differentiated in NB and switched to DMEM (D), or differentiated in DMEM and switched to NB medium (E). Media change was performed on day 1 after subculture (Red asterisk). Trends were confirmed across N=3 biological replicates.

Next, we wanted to confirm that these results were not due to possible mechanistic differences induced during differentiation, and that these effects were reversible. Indeed, differentiating and purifying BMECs in

DMEM, and then switching to NB medium 24 hours after removing bFGF and RA (i.e. 48 hours after subculture) resulted in a significant increase in TEER by ~2,000-4,000 Ω x cm^2 after 24 hours **(Figure 4E)**. Vice versa, if we differentiated in NB medium and then switched to DMEM, the typical TEER increase was halted to produce a TEER differential of >2,000 Ω x cm^2 **(Figure 4D)**. To confirm that this effect was not limited to changing media at a single, early time point, we instead changed from NB medium to DMEM, and vice versa, on 7 days after subculture. Accordingly, switching from DMEM to NB medium resulted in the same increase observed at the early time point, and the opposite scenario produced the same halt in TEER observed previously **(Figure 5)**. Thus, the basal medium used in BMEC differentiation plays a significant effect on passive barrier properties, and the BMECs are responsive to change in available nutrients at later time points after purification.

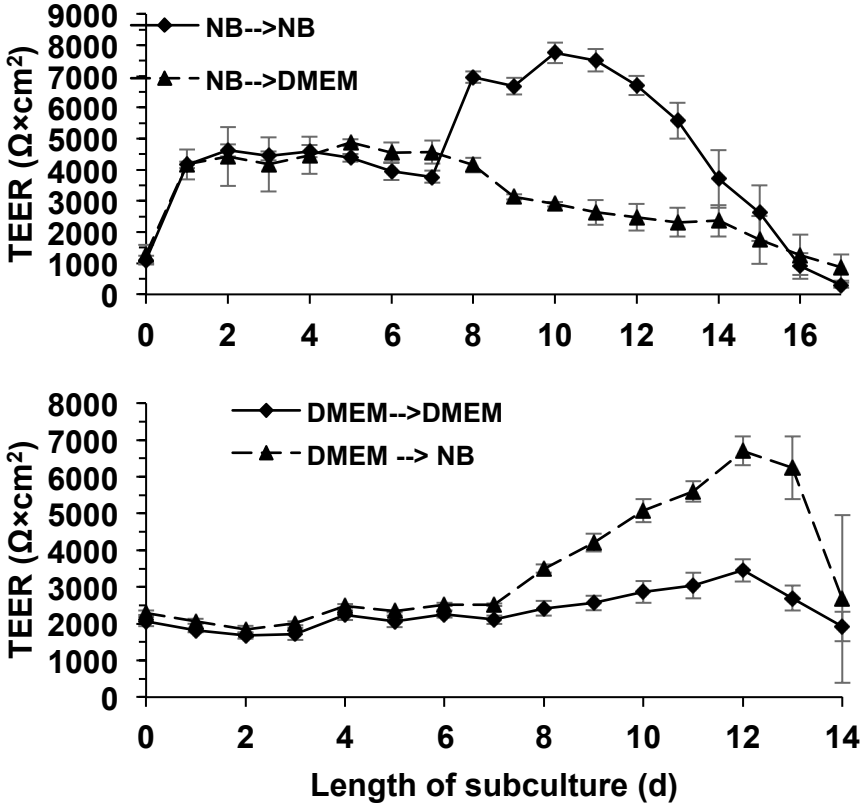

Figure 5. BMECs are responsive to media changes at later, mature time points. iPSC-derived BMECs were either differentiated in NB and switched to DMEM (top panel) or differentiated in DMEM and switched to NB (bottom panel). Media was changed on day 7 after purification and trends were confirmed across N=3 biological replicates.

3.3b. Basal medium does not affect passive permeability to sodium fluorescein and efflux activity

Despite the remarkable TEER differences observed between BMECs differentiated in DMEM compared to NB medium, previous reports suggest that above a certain TEER threshold, there will not be any functional differences. As such, we investigated whether permeability to the tracer molecule sodium fluorescein differed between BMECs differentiated in NB medium and DMEM. While our data indicates that iPSC-derived BMECs cultured in DMEM are less permeable than when cultured in NB medium, both have effective permeability's in the same range as BMECs in hESFM with B27 or ITS, indicating a low paracellular permeability **(Figure 6A)**. Since one of the main differences between DMEM and NB medium is amino acid concentration, we posited that amino acid metabolism could be responsible for the TEER differential (further details in chapter 4). Therefore, we investigated whether removal of amino acids from NB medium would alter P_e. The results suggest that there is not difference in permeability when amino acids are removed from NB medium and agree with the previous observation that permeability is not effected above a TEER threshold[48]. Further, basal media composition did not influence the p-glycoprotein activity **(Figure 6B)**, suggesting that only passive barrier characteristics are influenced.

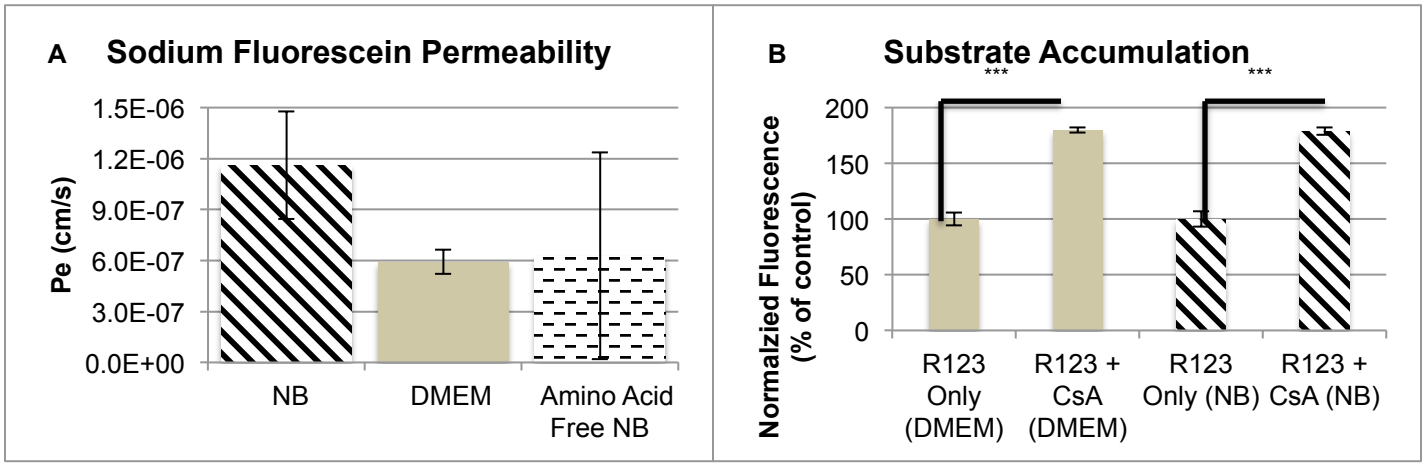

Figure 6. Fully characterizing barrier properties. A) Effective permeability of sodium fluorescein for CC3-derived BMECs when differentiated in NB medium, DMEM, or NB medium then switched to amino acid free NB 48 hours after purification. **B)** Intracellular fluorescence accumulation was measured in CC3-derived BMECs cultured in DMEM or NB medium and incubated with PGP substrates and inhibitors. Data represents technical N=3 from a single biological sample and subjected to a student's t-test for statistical significance. (*** $p<0.001$)

3.3c. Searching for the components causing the TEER differential between DMEM and NB medium

As discussed in section 3.3a, the basal medium in which BMECs were differentiated in has a significant impact on the maximum TEER achieved. When BMECs were differentiated in DMEM, TEER generally reached a maximum of ~1,000-2,000 Ω x cm^2; however, when differentiated in NB medium, TEER reached a maximum that exceeded 8,000 Ω x cm^2. Interestingly, these media are composed of most of the same compounds, varying only slightly in the concentrations of some amino acids and vitamins. Furthermore, our own preliminary evidence from high throughput metabolomics suggests that amino acid metabolism is significantly altered when passive barrier function increases in response to RA treatment **(Figure 7A)**. Thus, we initially hypothesized that the BMECs were utilizing amino acids to meet their bioenergetics demands, and that DMEM was lacking key amino acids that prevented BMECs from reaching TEER maximum observed in BMECs differentiated in NB. To investigate this hypothesis, we differentiated and purified BMECs in either DMEM or NB medium, then changed to medium supplemented with, or lacking compound(s) of interest.

Previous work has implicated the importance of branched-chain amino acid (BCAA) metabolism in neurodegenerative disease[50-55]. The BCAAs (leucine, isoleucine, and valine) are collectively ~8-fold lower in DMEM than NB medium. Taken together, we first probed whether the removal of BCAAs from NB medium reduced TEER to levels found from BMECs in DMEM. However, there was no loss in barrier function as measured by TEER when BMECs were switched from NB medium to NB medium that lacked BCAAs **(Figure 7B)**. We then took this a step further and removed all of the amino acids from NB medium after differentiation and purification. Remarkably, these BMECs maintain a high TEER, similar to the maximum values seen in BMECs in NB, and maintained a stable barrier for the same duration that was observed in BMECs in the control NB medium **(Figure 7B)**. This suggests that the difference in amino acids is not likely to be the cause of the TEER plasticity.

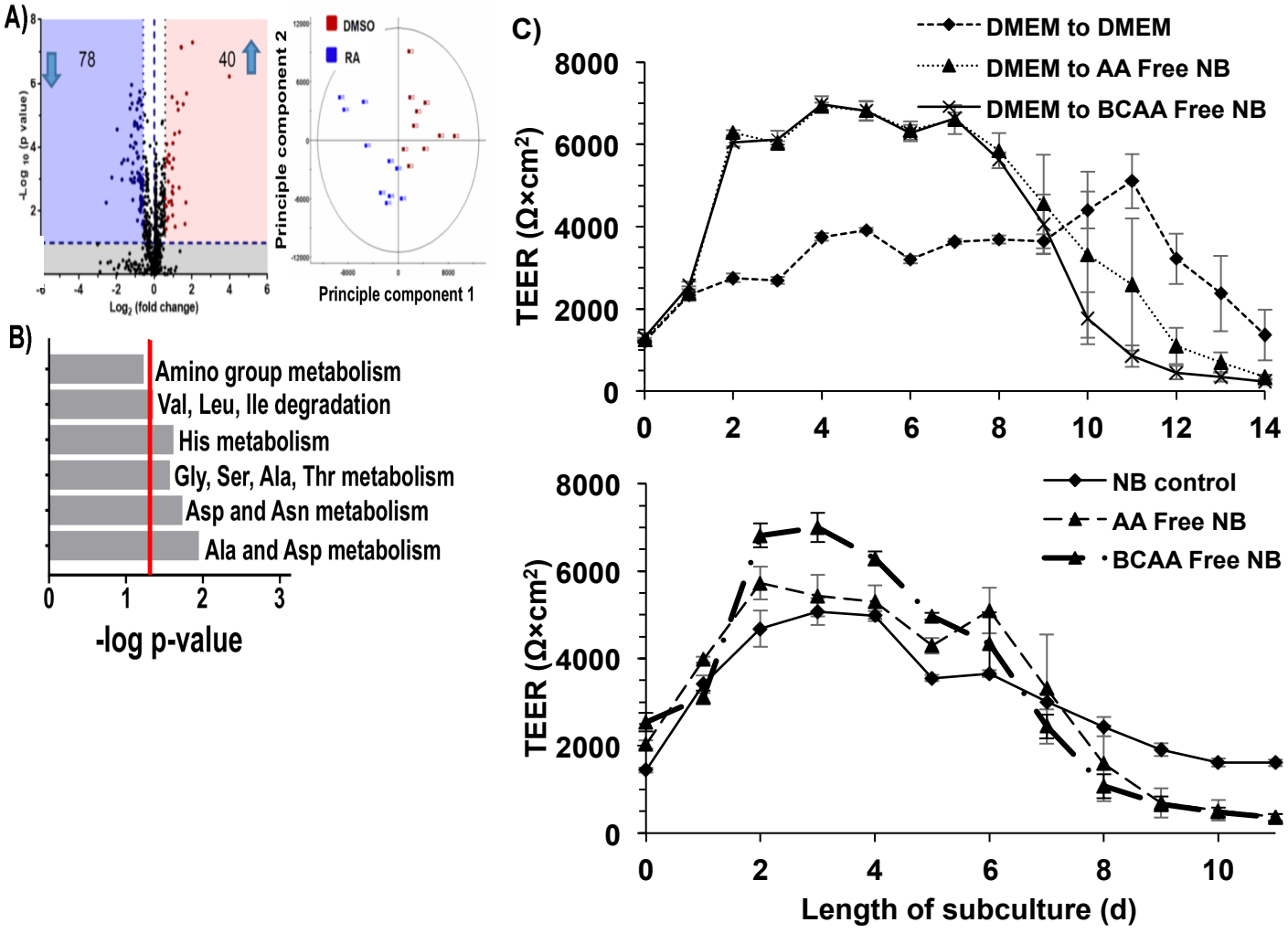

Figure 7. iPSC-derived BMECs yield a high-fidelity barrier when cultured in amino acid free NB medium. A) Untargeted metabolomics in iPSC-derived BMECs show differential metabolite profile when BMECs are subjected to RA treatment to increase passive barrier function. B) Statistically altered pathways due to RA treatment suggest altered amino acid metabolism. C) iPSC-derived BMECs differentiated in DMEM (top) or NB medium (bottom) then switched to amino acid-free or branched-chain amino acid-free NB medium respond similarly to BMECs in NB medium.

With our interest in metabolism, we further investigated the importance of glucose in the media if amino acids were present. We differentiated and purified BMECs in DMEM or NB medium, then switched to media containing either 0 mM (GF NB), 25 mM (the normal amount in NB medium), or 125 mM glucose (HG NB). BMECs in each media condition maintained high passive barrier function as measured by a high TEER **(Figure 8)**, with BMECs in 125 mM glucose slightly increasing TEER compared to the other three conditions. We postulate that while BMECs are in media with lower glucose concentrations, they primarily utilize amino

acids; however, this balance shifts and BMECs may utilize both glucose and amino acids when in high glucose media. Taking a closer look at the compositions of DMEM and NB medium, we recognized that many of the vitamins, specifically those that are part of the vitamin B family, are elevated in NB medium compared to DMEM. Additionally, many of these vitamins are important cofactors in ox-phos reactions. As such, we hypothesized that by adding vitamins to DMEM so they were at the same concentration as in NB medium **(Table 2)** we could close the TEER differential between DMEM and NB medium. However, supplementing DMEM with the vitamins failed to produce the TEER increase that BMECs typically have when cultured in NB medium **(Figure 9).** Further attempts to elucidate the mechanisms involved that contribute to the TEER differences between BMECs in DMEM and NB are discussed in chapter 4.

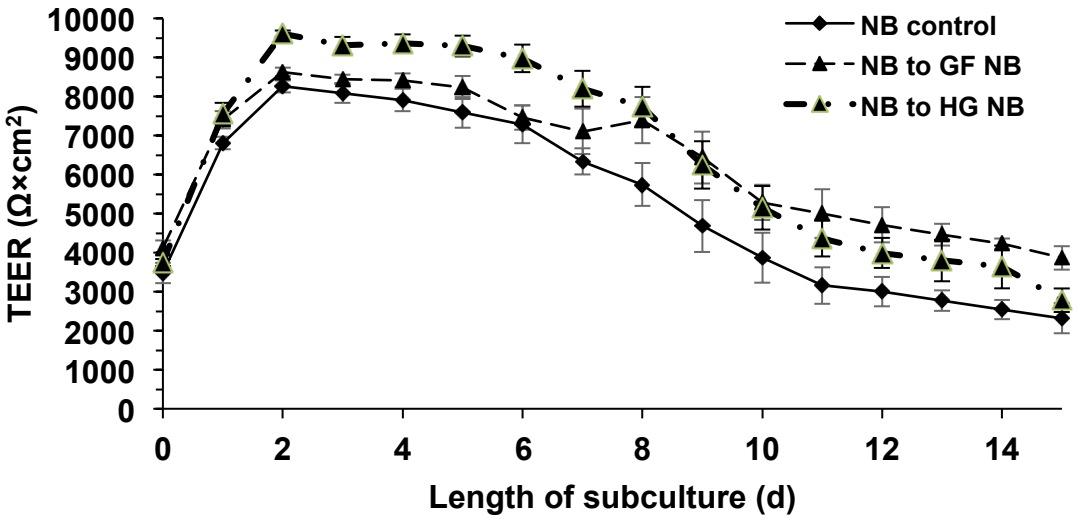

Figure 8. BMECs are cultured in NB medium without glucose (GF NB) or 125 mM glucose (HG NB). TEER plot for iPSC-derived BMECs differentiated and purified in NB medium, then switched to NB medium 125 mM glucose, or glucose free NB medium on day 1 after subculture.

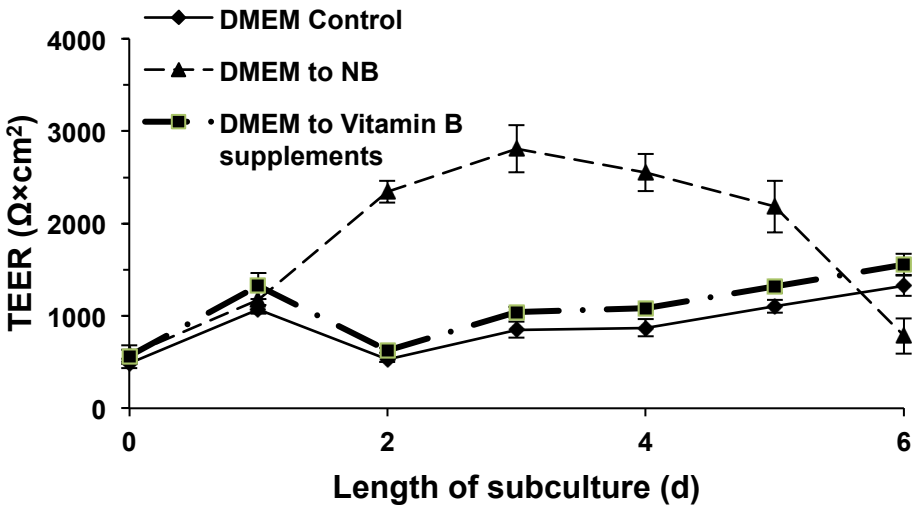

Figure 9. BMECs are cultured in DMEM and supplemented with vitamins. BMECs differentiated and purified in DMEM are switched to NB medium or DMEM supplemented with vitamins at the concentrations present in NB

Table 1: Composition of DMEM and NB medium.

	ALL VALUES IN mg/L		
COMPONENT	**DMEM/F12**	**NB**	**% CHANGE**
Glycine	18.75	30	60%
L-alanine	4.45	2	-55%
L-arginine hydrochloride	147.5	84	-43%
L-asparagine	7.5	0.83	-89%
L-aspartic acid	6.65	0	-100%
L-cysteine hydrochloride	17.56	31.5	79%
L-cystine 2HCL	31.29	0	-100%
L-glutamic acid	7.35	0	-100%
L-glutamine	365	0	-100%
L-histidine hydrochloride	31.48	42	33%
L-isoleucine	54.47	105	93%
L-leucine	59.06	105	78%
L-lysine hydrochloride	91.25	146	60%
L-methionine	17.24	30	74%
L-phenylalanine	35.48	66	86%
L-proline	17.25	7.76	-55%
L-serine	26.25	42	60%
L-threonine	53.45	95	78%
L-tryptophan	9.02	16	77%
L-tyrosine	55.79	72	29%
L-valine	52.85	94	78%

biotin	0.0035	0	
choline chloride	8.98	4	
D-calcium panthothenate	2.24	4	
folic acid	2.65	4	
niacinamide	2.02	4	
pyridoxine hydrochloride	2.013	4	
riboflavin	0.219	0.4	
thiamine hydrochloride	0.17	4	
vitamin B12	0.68	0.0068	
i-Inositol	12.6	7.2	
calcium chloride	116.6	200	
cupric sulfate	0.0013	0	
ferric nitrate	0.05	0.1	
ferric sulfate	0.417	0	
magnesium chloride	28.64	77.3	
magnesium sulfate	48.84	0	
potassium chloride	311.8	400	
sodium bicarbonate	2438	2200	
sodium chloride	6995.5	3000	
sodium phosphate dibasic	71.02	0	
sodium phosphate monobasic	62.5	125	
zinc sulfate	0.432	0.194	
D-glucose	3151	4500	
hypoxanthine	2.39	0	
Linoleic acid	0.042	0	
Lipoic acid	0.105	0	
phenol red	8.1	8.1	
putrescine	0.081	0	
sodium pyruvate	55	25	
thymidine	0.365	0	

Table 2: Vitamins added to DMEM medium.

	ALL VALUES IN mg/L	
COMPONENT	**DMEM/F12**	**NB**
D-calcium panthothenate	2.24	4
folic acid	2.65	4
niacinamide	2.02	4
pyridoxine hydrochloride	2.013	4
riboflavin	0.219	0.4
thiamine hydrochloride	0.17	4

3.4. Discussion

The goal of this work was to identify critical compounds in NB medium that were responsible for BMECs increased TEER when cultured in NB medium compared to when BMECs are cultured in DMEM. Considering that DMEM has >50 components, and NB has >35 components **(Table 1)**, this represented a tremendous undertaking. Previous work suggested that amino acid metabolism is altered between BMECs with increased passive barrier function relative to BMECs without a high-fidelity barrier, we hypothesized that amino acid metabolism differed between BMECs in DMEM and NB medium. However, when we adjusted the amino acid content of NB medium to reflect that of DMEM, BMECs did not respond accordingly. Furthermore, removal of BCAAs from NB medium—reflecting the decrease in BCAA concentration in DMEM—did not affect the TEER. Intriguingly, complete removal of amino acids from NB medium did not cause BMEC TEER to drop to levels observed when BMECs are in DMEM. In fact, TEER did not drop at all when amino acids were removed from the medium.

We then shifted our focus to the vitamins in the media. **Table 2** details the vitamins that were both added to, and removed from the media. We specifically focused on a group of six vitamins that are present in both DMEM and NB media, but are elevated in NB. These six vitamins are also all part of the vitamin B family and are important cofactors in numerous oxidative metabolic reactions. As such, we suspected that the combined elevated levels in NB medium could enhance some unknown pathways in BMECs that contributes to the increased TEER. However, we failed to see any difference when we increased the concentration of these vitamins in DMEM to their concentrations found in NB medium. It is possible that there is a specific combination of amino acids, vitamins, and/or inorganic compounds responsible for the elevated TEER observed when BMECs are in NB medium. While we have began to explore a variety of custom media formulations investigating different combinations, the time required to make and examine each media formulation has limited our throughput and, as such, these experiments are still a work in progress. Nevertheless, this work demonstrates BMEC's remarkable ability to adapt to the presence and absence of different nutrients while maintaining their high barrier function. This function is crucial *in vivo*; the BBB must remain intact under different stresses to protect the CNS and ultimately help protect against neurodegeneration.

Chapter 4: Defining Metabolic Pathways in BMECs

4.1. Introduction

Metabolic pathways have been studied in cells for over 100 years, yet new insights are constantly emerging into how specific cell types use different fuel sources to carry out their specialized roles in the body. For instance, although endothelial cell metabolism has been studied for several decades[24], a new report was published in 2018 detailing how fatty acid oxidation can dictate endothelial-to-mesenchymal transitions through maintenance of acetyl-CoA levels in peripheral vascular beds[56]. However, very little emphasis has been placed on BBB metabolism. Given the recent advancements in iPSC-derived BMEC models, including our own newly published model[57] (detailed in chapter 2), we are more adept than ever before to study the influence of specific cues on BBB function since the system can be fully specified and analyses of the extracellular milieu will not be confounded by serum. Furthermore, our preliminary data has implicated cellular metabolism as a cause in differential barrier properties identified in BMECs under a variety of conditions. As such, we sought to expand on the differences that arise from changes in basal media composition by identifying specific pathways utilized under each condition. The work detailed in chapter 3 suggests that BMECs are metabolically flexible, with the ability to utilize different nutrient sources to meet their bioenergetics demands. Using cutting-edge techniques, including metabolic profiling with the label-free Seahorse XFe metabolism assay and super-resolution imaging, we have begun to characterize metabolic status in BMECs and demonstrate the metabolic function may have profound influences on the barrier function. We sought to identify which metabolic pathways are primarily used under basal conditions, and characterize how this changes under potentially environmental stressors such as glucose or amino acid deprivation. This work could reveal novel aspects of BBB regulation that could have important implications for neurovascular disease progression and treatment.

4.2. Experimental Design

4.2a. Differentiation of generic iPSC-derived ECs

iPSCs are maintained in E8 medium[41], prepared in-house as previously described[39], on growth factor reduced Matrigel. When iPSCs were 60-80% confluent, the cells were washed once in DPBS and incubated in Accutase for 3-5 minutes at 37°C. The resultant single cell suspension was collected via centrifugation, resuspended in fresh E8 medium containing 10 μM of the ROCK inhibitor Y-27632. Cells were counted using Trypan blue cell viability assay and seeded at a density of ~50,000 cells/cm^2. The following day, media was changed to E6 medium supplemented with 4 μM of CHIR99021, a potent Wnt pathways activator, to induce differentiation. After two days of treatment with CHIR99021, media was changed to E6 lacking CHIR99021. Media was changed daily for the next 3 days. Next, cells were subjected to a magnetic activated cell sort (MACS) to purify CD34+ endothelial progenitor cells. Briefly, cells were washed once with DPBS and incubated in Accutase for 5-10 minutes at 37°C. The resultant single cell suspension was passed through a 40 μM mesh cell strainer to remove remaining clumps of cells. The strained cells were collected via centrifugation and resuspended in MACS buffer (5 mg/mL bovine serum albumin in DPBS with 5 mM EDTA), F_c blocker, and CD34 microbeads and incubated for 30 minutes at 4°C. After 30 minutes, cells were washed once with MACS buffer, centrifuged to recollect, and resuspended in MACS buffer. The resultant cell solution was added to a MS MACS column on a magnet to separate the CD34+ cells. Once the buffer had passed through the column, MACS buffer without cells was passed through three times to wash the column and remove any nonspecific cells that bound. Next, the column was removed from the magnet and cells were collected from the column in MACS buffer. The cells suspension was collected via centrifugation, resuspended in E6 media containing 10 μM ROCK inhibitor, and seeded at a density of ~25,000 cells/cm^2 on collagen coated plates. The following day E6 was replaced with hESFM supplemented with 1% PDS. Media was changed every 2-3 days.

4.2b. Culture of hCMEC/D3s and bovine BMECs

hCMEC/D3 cells were maintained in EndoGro-MV complete culture medium (EndoGRO basal medium containing L-glutamine, 5% fetal bovine serum, EndoGRO-LS supplement, rhEGF, ascorbic acid, and bFGF) on collagen 1 coated plates. Medium is changed every other day until cells ~80% confluent.

Bovine BMECs were maintained in bovine BMEC growth media on fibronectin coated tissue culture plates and passaged when 60-80% confluent. For YSI assays, bovine BMECs were split in to three wells of a 12-well tissue culture plate and grown to confluence. When bovine BMECs reached confluence, media was changed to bovine BMEC basal medium and media collection began. Cells were used from passage number 2-10.

4.2c. Glucose consumption assays utilizing the YSI glucose/lactate analyzer

In previous experiments described in chapter 3, we discovered that BMECs could not only survive, but maintain a TEER >8,000 Ω x cm^2 in NB medium lacking either glucose or all amino acids. We hypothesized that BMECs preferentially utilize amino acids, but shift towards glucose metabolism when deprived of amino acids. We used the YSI glucose/lactate analyzer to measure how much glucose cells consumed from the medium under each condition, and to measure how much lactate these cells produced. iPSC-derived BMECs were differentiated as previously described and followed the altered timeline described in chapter 3. Briefly, BMECs from one well of a 6-well plate were purified on to three wells of a 12-well tissue culture plates coated with collagen and fibronectin solution substrate, and BMECs were cultured in the basal medium supplemented with bFGF and RA for 24 hours. bFGF and RA were then removed from the basal medium for another 24 hours. The next day, medium was changed a second time to DMEM, NB medium, or the desired altered medium (e.g. NB medium lacking amino acids). At this point, 100 µL of media were collected per well (with 3 wells per condition), and this represents T = 0 hours.. 100 µL of media was collected from each well at 6, 12, 24, and 48 hours following the initial collection. Each sample was collected and stored at -80°C until all samples were collected. iPSC-derived generic ECs were cultured as described above. When they reached ~70% confluence, media was changed to fresh hESFM with 1% PDS and media collection began. Similarly, hCMEC/D3s were cultured as described above, and split from one well of a 6 well plate to three wells of a 12-

well plate. Once the cells reached ~80% confluence, the media was changed to fresh EndoGRO-MV medium and media collection began. Furthermore, for every condition, media was also collected from a well that was cell-free. This accounts for any glucose and lactate concentration changes due to evaporation over the course of 48 hours.

After all samples were collected, cells were fixed in 4% PFA as described previously, incubated with DAPI for 10 minutes, and imaged. 4 fields per well, for a total of 12 fields per condition, were captured and cells were counted using ImageJ. Once all samples were collected, they were thawed and ran on the YSI. Each sample was measured twice for a total of 6 measurements per condition per time point (3 technical replicates per condition, times 2 measurements per sample). The average of the 6 measurements was calculated and normalized to the cell count to obtain the glucose and lactate concentrations. These concentrations were then normalized to the cell-free conditions to account for changes due to evaporation. Finally, we calculated the average and maximum rates of glucose production/lactate production for each condition on a per cell basis.

4.2d. Seahorse XFe96 label-free, live-cell metabolism assays

iPSC-derived BMECs were differentiated as previously described, and subcultured onto 96-well tissue culture plates that are uniquely designed for the Seahorse XFe96 instrument. iPSC-derived BMECs were subcultured at a density of ~50,000 cells per well to ensure a confluent monolayer formed. Media was changed using the same timeline described in section 4.2a, and the assay was carried out 24 hours after the final media change (i.e. 72 hours after BMEC purification). On the day of the assay, the basal media of interest is removed and replaced with assay medium—DMEM/F12 supplemented with glucose, L-glutamine, and pyruvate and incubated at 37ºC in a CO_2 free incubator for 1 hour to remove CO_2 from the cells, as this interferes with pH and H+ measurements. We conducted the cell-mito stress test to assess how BMECs responded when mitochondrial metabolism was inhibited by injection of compounds at various time points. This assay measures extracellular acidification rate (ECAR) and oxygen consumption rate (OCR), which corresponds to whether the cell is utilizing glycolysis (ECAR) or oxidative metabolism (OCR). Baseline metabolism was measured 3 times, and metabolic status was measured three times following each injection. First, oligomycin is injected to inhibit

ATP-synthase in order to determine non-mitochondrial oxygen consumption. Next, the mitochondrial uncoupler trifluoromethoxy carbonylcyanide phenylhydrazone (FCCP) is injected to determine the maximum OCR. Finally, a mixture of rotenone and antimycin A is injected, inhibiting mitochondrial complexes I and III, effectively shutting down mitochondrial respiration. After each injection, the media is mixed briefly prior to measuring each sample. After the assay, cells were fixed in 4% PFA, stained with DAPI and imaged for a cell count. All data were normalized to the number of cells, and recorded as mean ECAR, OCR, or ATP ± standard deviation.

4.2c. Structured illumination microscopy

iPSC-derived BMECs were subcultured on to collagen and fibronectin coated Matek tissue culture plates in the basal media of interest (DMEM or NB) supplemented with bFGF and RA. 24 hours after 'barrier induction' via the removal of bFGF and RA, media was removed and replaced fresh media containing 1 nM Mitotracker Red for 30 minutes. Cells were then washed three times in PBS and fixed in 4% PFA. The cells were stained following the same parameters described in section 2.2c and imaged on a Nikon SIM super resolution microscope. Images were reconstructed on Nikon Elements software, and all analyses were conducted on ImageJ and Nikon elements.

4.3. Results

4.3a. Glucose consumption rates vary with basal media conditions

We used the YSI glucose/lactate analyzer to investigate how much glucose iPSC-derived BMECs consumed and how much lactate these cells produced when cultured in NB medium at two different glucose concentrations. Furthermore, we compared this with the rates in primary bovine BMECs, hCMEC/D3 cells, and iPSC-derived generic ECs. The iPSC-derived BMECs consumed about the same amount of glucose (~1.25 nM/cell) when cultured in either the NB control medium or the 5 mM euglycemic NB medium. Likewise, the iPSC-derived generic ECs and hCMEC/D3 consumed similar amount of glucose on a per cell basis. (~2-2.5 nM glucose/cell) **(Figure 10)**. It is interesting to note that the hCMEC/D3 immortalized cell line and the iPSC-

derived generic ECs were very similar in terms of glucose consumed and lactate produced. ECs throughout the peripheral vasculature are typically glycolytic, as are immortalized cell lines. Finally, the bovine BMECs results differed most from the other cell types but we determined that these bovine BMECs formed a very low fidelity barrier (TEER <500 Ω x cm^2), suggesting that they are not BBB-like and may have properties more similar to peripheral ECs when cultured *in vitro*.

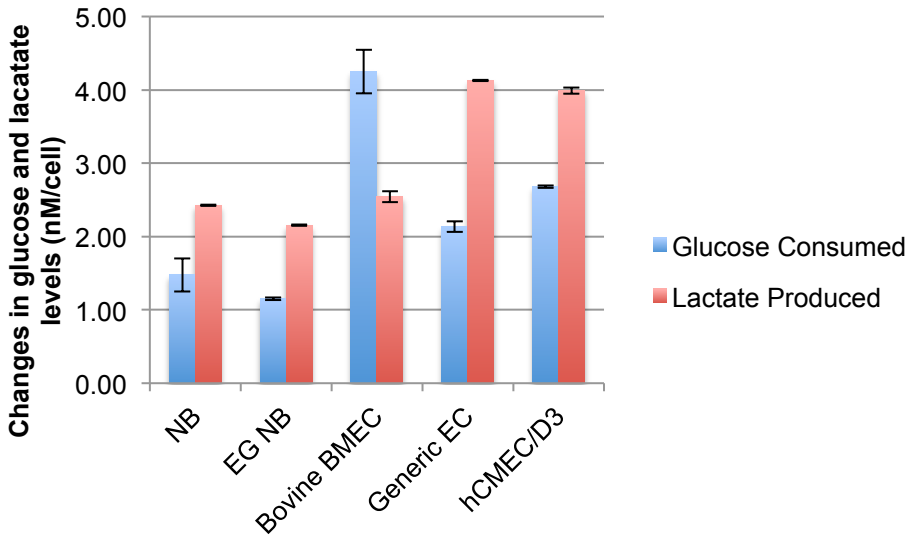

Figure 10. Change in glucose and lactate levels in different types of endothelial cells after 48 hours. Media was collected and ran on a YSI glucose/lactate analyzer to determine different endothelial cell types utilized glucose from N=3 technical replicates from a single biological sample. EG NB: euglycemic NB (5 mM glucose). Concentrations represent the difference in glucose and lactate in the media between T=0 and T=48.

We then further examined if altering the glucose concentration or removing amino acids from NB medium affected glucose consumption and lactate production. First, BMECs in NB medium with 1 mM glucose consumed the entire 1mM of the glucose within ~12 hours, consistent with the amount of glucose consumed during the same duration when BMECs are cultured in NB medium **(Figure 11B)**. As expected, lactate production plateaued in this low glucose condition after about 24 hours **(Figure 11C)**. Surprisingly, BMECs cultured in amino acid free NB medium consumed glucose at a significantly lower average and maximum rate than BMECs in 25 mM (control) NB medium **(Figure 11)**. However, neither the rates in lactate production nor the total lactate produced differed between these two samples **(Figure 11A)**. We also cultured the BMECs in

NB medium containing 125 mM glucose. While this glucose concentration was out of range for the YSI to measure, we were still able to obtain lactate measurements. We found that culturing BMECs in high glucose NB medium did not alter the total lactate levels or the lactate production rates **(Figure 11A,C)**.

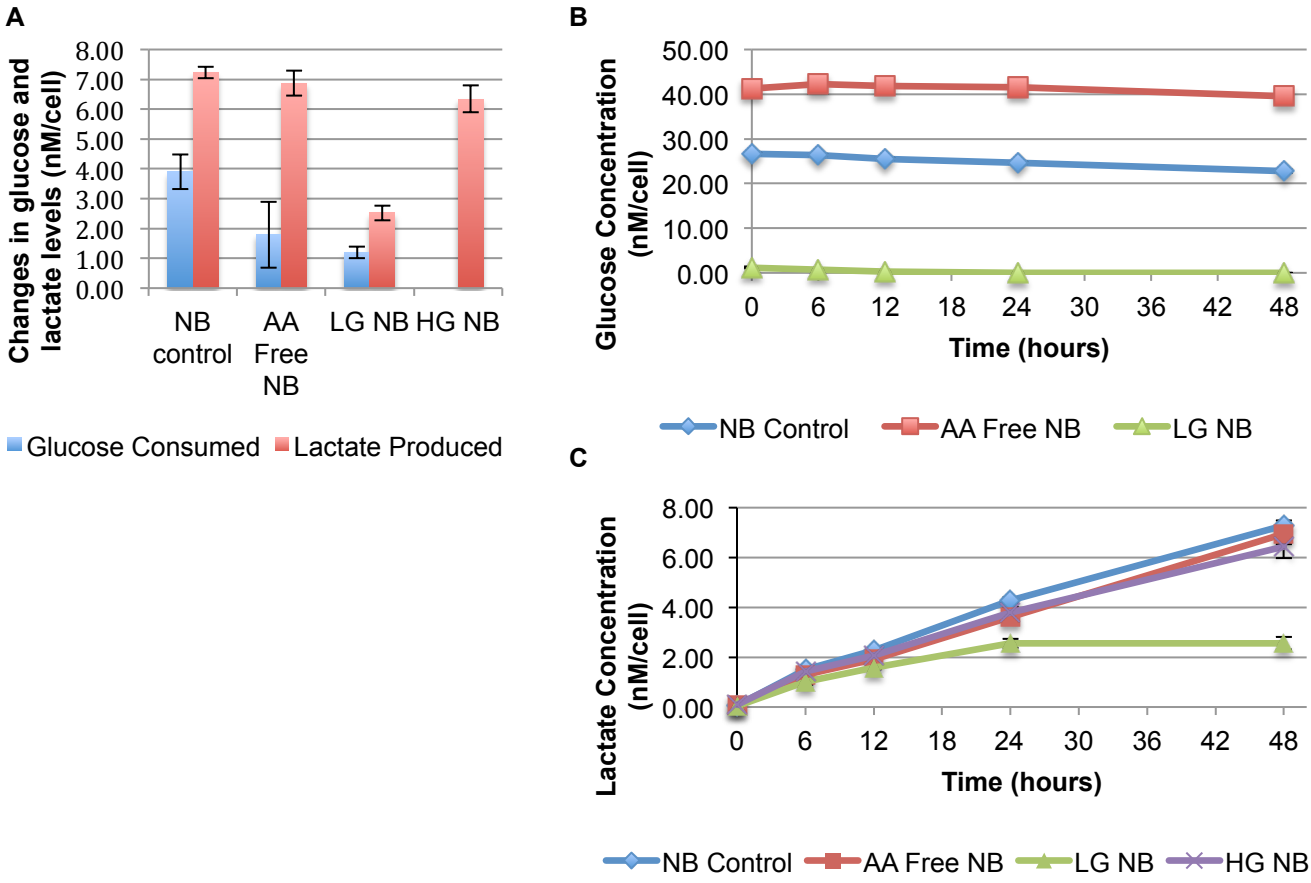

Figure 11. Changes in glucose and lactate levels after 48 hours in various media compositions. BMECs were cultured in NB media with a variety of glucose and amino acids to assess how nutrient abundance influenced metabolic pathway preference. **A)** The difference in glucose and lactate concentrations in the media between T=0 and T=48. **B)** Hourly glucose usage when iPSC-derived BMECs are cultured in each media. **C)** Hourly lactate production when iPSC-derived BMECs are cultured in each media.

We next investigated how the hexokinase II (HKII) inhibitor 3-bromopyruvate (3-BP) affected glucose consumption and lactate production when BMECs were cultured in NB medium. Interestingly, TEER dropped slightly compared to the untreated control 24 hours after 3-BP was added (**Figure 12A**). This differential only occurred for 24 hours, as the TEER of 3-BP treated cells rebounded to the same level as untreated cells after another 24 hours and remained at the same level for the duration of the experiment. This effect also occurred

in BMECs cultured in DMEM **(**data not shown**)**. Thus, although this is not unique to the basal media BMECs are cultured in, further investigation could provide insight into basal BMEC metabolic properties. Accordingly, we collected media from BMECs cultured in NB medium with or without 3-BP for the same duration as the previous YSI assays. However, despite the TEER differential observed between 0 and 24 hours, there was no difference in glucose consumption or lactate production between 3-BP treated and control BMECs across any period of time measured **(Figure 12B-C)**.

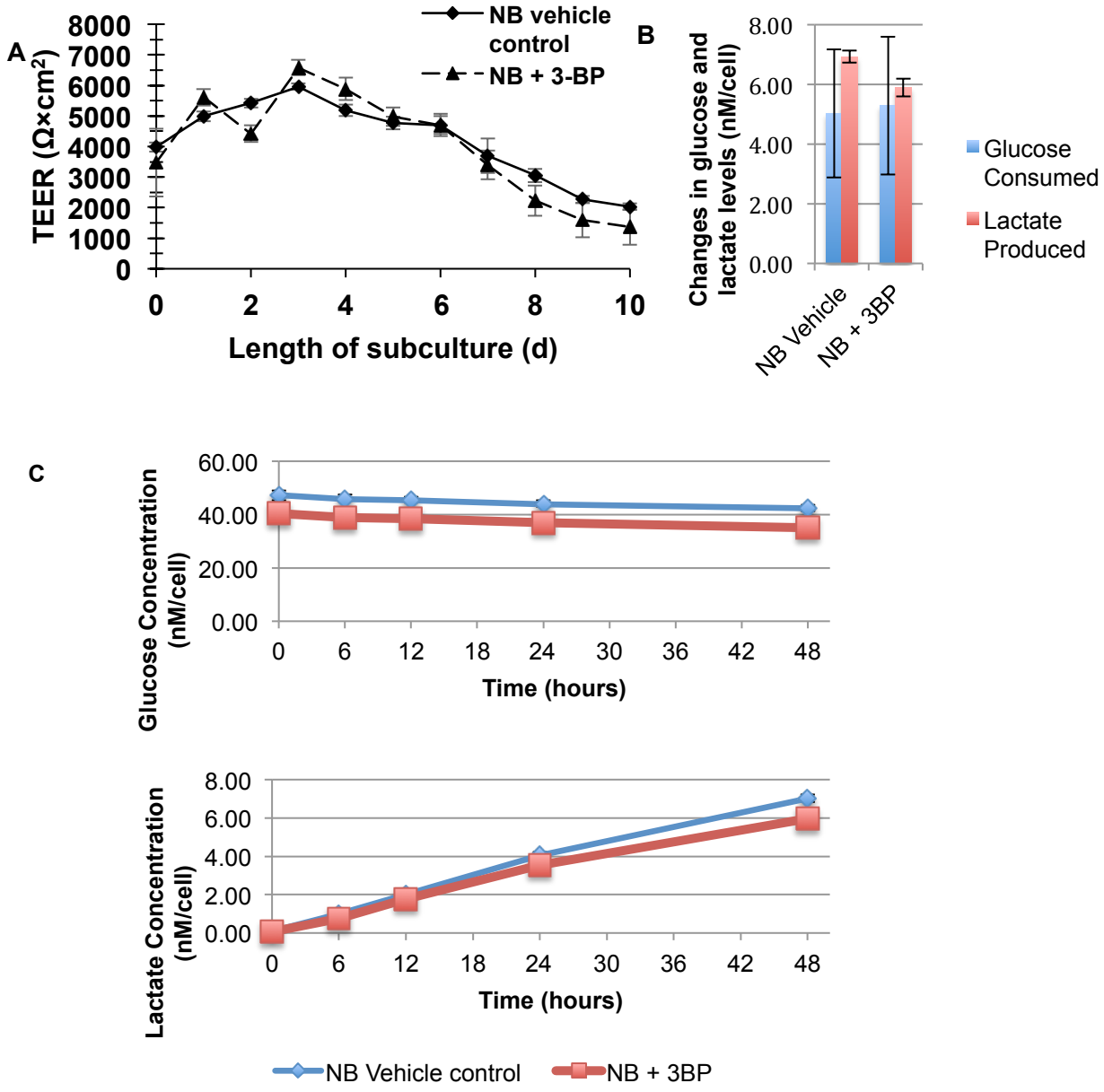

Figure 12. YSI glucose/lactate analyzer was used to measure glucose and lactate usage in presence of glycolysis inhibitor. A) TEER plot of BMECs cultured in NB. Media was changed on Day 1 to include the inhibitor 3-BP or vehicle control. **B)** Changes in glucose and lactate levels after 48 hours of culture. **C)** Hourly plot of glucose and lactate usage.

4.3b. Seahorse assay suggests BMEC basal metabolism may differ when in DMEM compared to NB medium

We hypothesized that a driving force producing the TEER differential observed when BMECs are cultured in DMEM and NB medium was a difference in amino acid metabolism that led to altered metabolic status in when BMECs were cultured in DMEM. To test whether the BMECs utilized different pathways (glycolysis vs ox-phos), and to investigate how BMECs responded to mitochondria stress, we used the Seahorse XFe96 to assess live-cell metabolic status. Further, we posited that BMECs cultured in DMEM would produce less ATP compared to BMECs cultured in NB medium and would be more sensitive to the addition of inhibitors. However, this hypothesis was rejected, as BMECs in DMEM actually had an OCR greater than BMECs in NB, regardless of whether they were initially differentiated in DMEM or NB medium **(Figures 13 and 14)**. In fact, when BMECs were differentiated, purified, and then stayed in DMEM, they had approximately twice the basal OCR than when switched to NB medium after purification **(Figure 14)**. Moreover, BMECs in DMEM produced slightly more ATP compared to BMECs in NB **(Figures 13 and 14)**. Additionally, BMECs responded to the injection of the inhibitors in a similar manner, suggesting that mitochondria are not more susceptible to dysfunction in either condition.

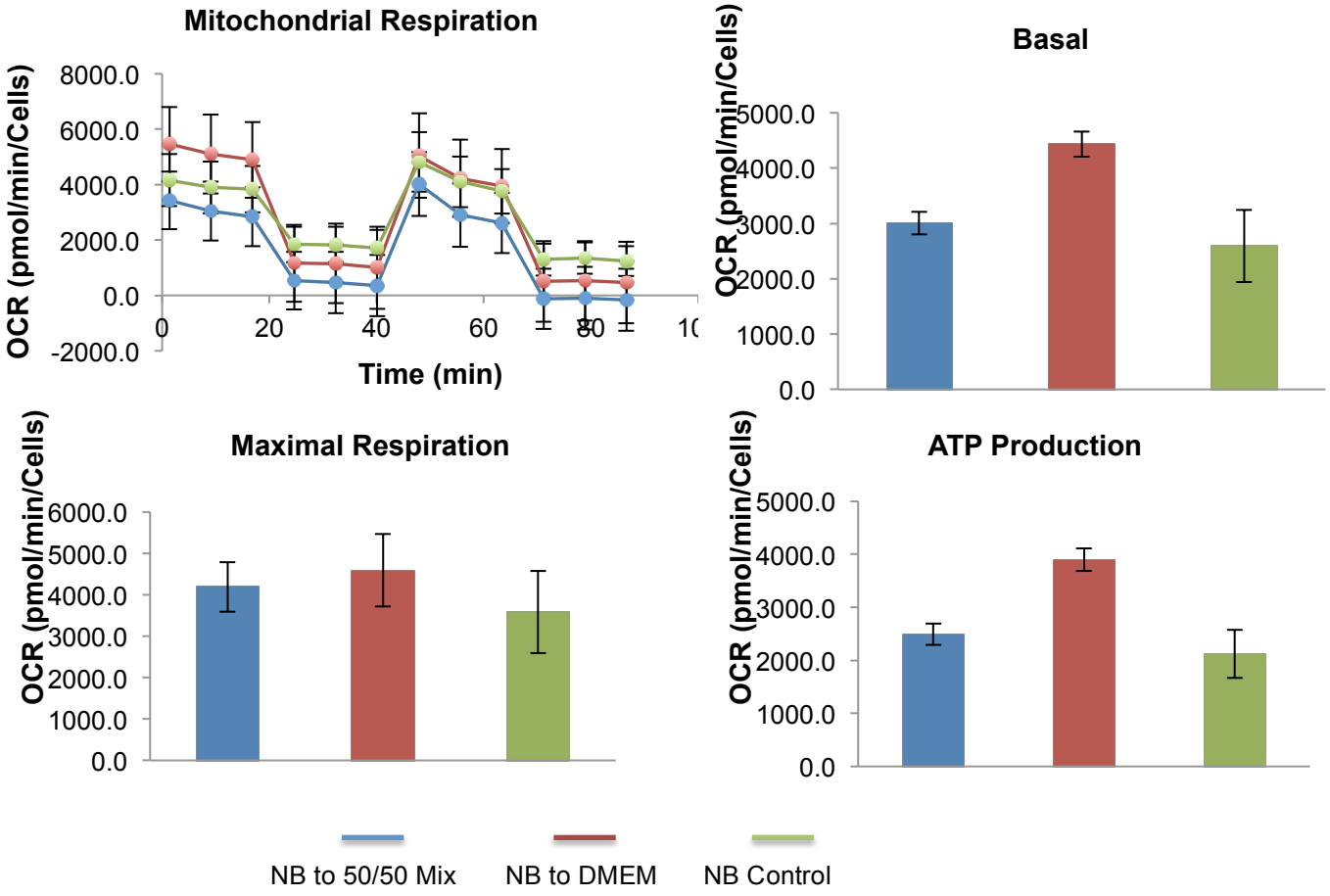

Figure 13. iPSC-derived BMECs were differentiated and purified in NB medium, then switched to either DMEM, a 50/50 mix of NB and DMEM, or NB medium after purification. Mitochondrial respiration is measured over a period of time in the presence of mitochondrial inhibitors and uncouplers. This permits the calculation of basal and maximum respiration, and ATP production.

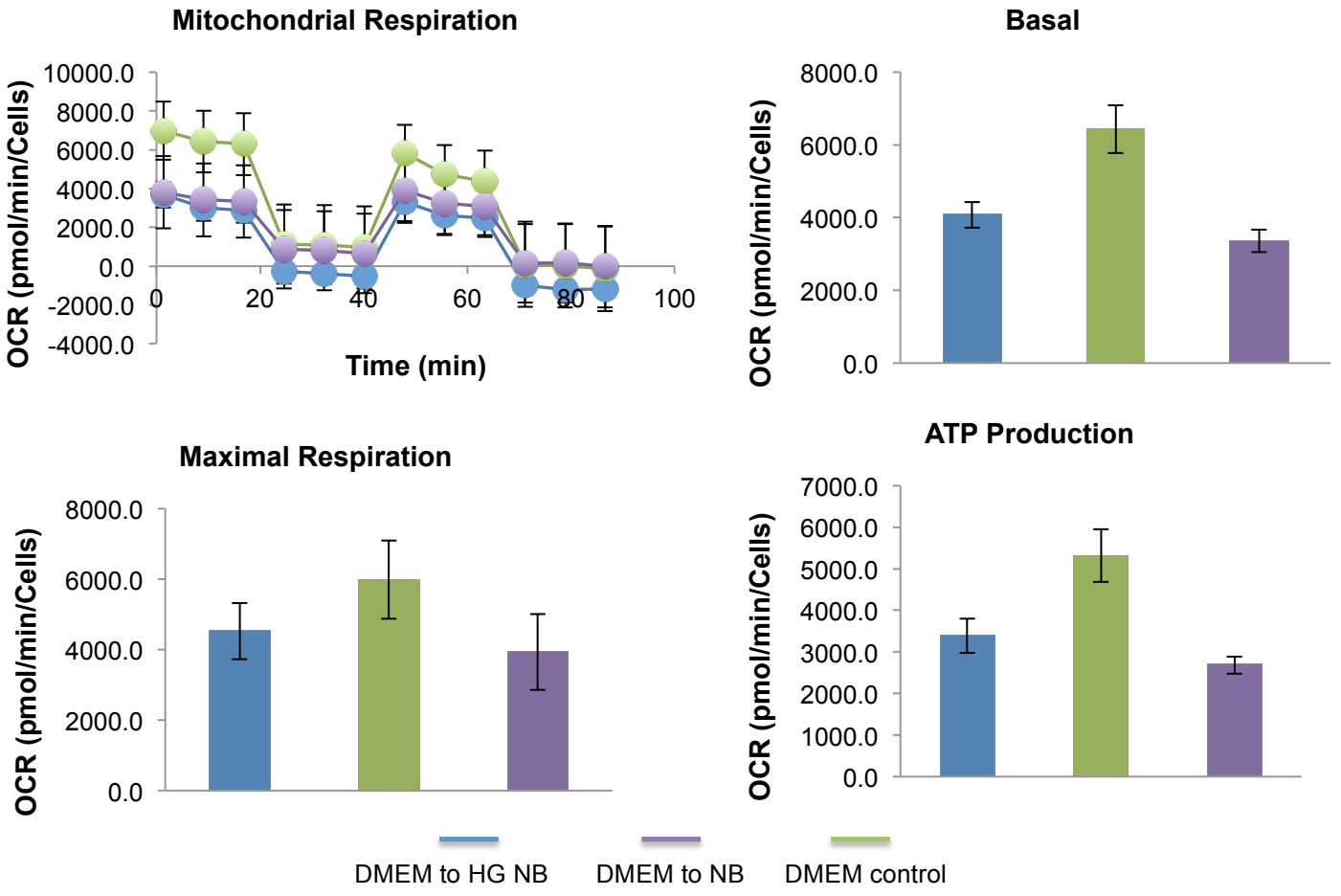

Figure 13. iPSC-derived BMECs were differentiated and purified in DMEM medium, then switched to either DMEM, NB medium, or high glucose (125 mM) NB medium after purification. Mitochondrial respiration is measured over a period of time in the presence of mitochondrial inhibitors and uncouplers. This permits the calculation of basal and maximum respiration, and ATP production.

4.3c. Super resolution imaging identified elaborate mitochondrial networks in iPSC-derived BMECs

Mitochondria structures are strongly associated with metabolic status in iPSCs[62-63]. To examine if the mitochondria structures differed when iPSC-derived BMECs were differentiated in DMEM and NB medium, we used structured illumination microscopy (SIM). We observed that the mitochondria form elaborate, elongated networks in BMECs in both conditions **(Figure 14)**. Finally, we treated BMECs with 3-BP for 24 hours at the same point that we previously observed the slight drop in TEER to see if there were any corresponding changes in mitochondria structure. However, as with the YSI data, there did not appear to be any differences in

mitochondria structure between 3-BP treated and control cells. Finally, amino acid free NB did not appear to alter mitochondrial structure.

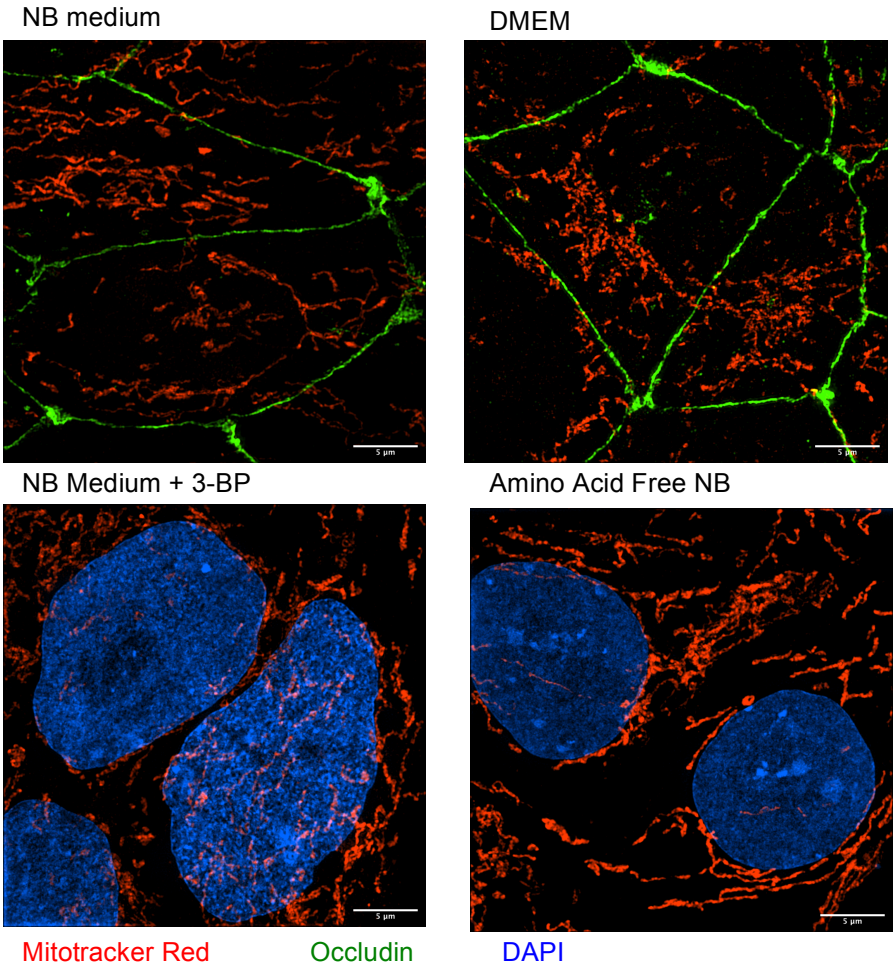

Figure 15. SIM images of iPSC-derived BMECs in different media conditions. iPSC-derived BMECs are cultured in DMEM, NB medium, NB medium with 3-BP, or amino acid free NB medium and incubated with the dye Mitotracker Red to stain mitochondria.

4.4. Discussion

Our preliminary and previous data strongly implicated altered metabolism as a key component driving TEER differences when BMECs are cultured in DMEM versus NB medium. As such, we sought to identify metabolic pathways and characteristics that differ between these conditions. Furthermore, there has not been much published work defining the general metabolic properties of BMECs. Therefore, this work aimed to

unravel unique features in BMECs that may point to differences in metabolism underlying BMECs specialized functions such as their barrier property. We used cutting edge metabolic profiling technique, super resolution imaging, and biochemical approaches to characterize BMEC metabolism.

Using the YSI glucose/lactate analyzer, we demonstrated that iPSC-derived BMECs consume very low amounts of glucose compared to iPSC-derived generic ECs and immortalized human BMECs. Furthermore, iPSC-derived BMECs produce low levels of lactate compared to iPSC-derived generic ECs and immortalized human BMECs. ECs throughout the peripheral system are generally considered to be highly glycolytic[25]. Furthermore, the process of immortalizing a cell line typically changes its properties such that they become highly glycolytic in their use of glucose as well. Thus, our data suggests that BMECs need less glucose than peripheral ECs to meet their bioenergetics demands, and much of the glucose in BMECs is oxidized completely in the mitochondria rather than utilized in glycolysis to produce lactate.

We then investigated whether lowering the concentration of glucose even further, significantly increasing the glucose concentration, or removing all amino acids from NB medium affected the amounts and rates of glucose and lactate consumed and produced. We hypothesized that hyperglycemic medium would force the BMECs towards glycolysis, and we would measure this by an increase in the total lactate produced and the rate at which it was produced. We further hypothesized that removal of amino acids as a source of fuel would cause BMECs to preferentially utilize glucose, likely via glycolysis. One significant caveat of this assay is that we cannot directly determine whether glucose is being utilized via glycolysis or being shunted to the mitochondria for oxidative metabolism. However, by comparing the amounts of glucose consumed and lactate produced across the different conditions, as well as our data from the Seahorse assay, we can make logical assumptions about how the BMECs are using glucose. Additionally, we inadvertently used a glucose concentration in the medium that was out of the measurable range of the YSI. While we are still able to gain valuable insight from the lactate levels, we cannot make any conclusions about the amount of glucose utilized and plan to rerun this with glucose levels that are elevated compared to control NB medium, but still within the YSI's range. As shown in **figure 10,** BMECs in the control (25 mM) NB had elevated rates of glucose consumption compared to the amino acid free NB and low glucose NB (1 mM). However, the BMECs in low glucose NB consumed all of the glucose within ~12 hours, and stopped producing lactate ~24 hours into the

experiment, indicating that BMECs will atleast partially utilize glycolysis to meet their bioenergetics demands. Intriguingly, removal of amino acids from NB medium seemingly caused BMECs to reduce the amount used and rate that they used glucose, while producing the same amount of lactate as both BMECs cultured in NB with 25 mM and 125 mM glucose. Additionally, increasing the glucose concentration to 125 mM did not cause lactate levels to increase. However, this data has not been replicated and should be considered very preliminary. Further replicates need to be completed to confirm that these trends are statistically significant.

We suggest a few plausible explanations for these phenomena. First, we believe that the BMECs may enter a 'survival' state when they sense that all amino acids are absent, preferentially shutting off all mitochondrial metabolism. Doing so forces the BMECs to utilize a non-preferred route of metabolism in glycolysis, and consequently using less glucose because none of the glucose is being oxidized in the mitochondria. With regards to the observation the BMECs produce the same amount of lactate when cultured in hyperglycemic NB medium, we suggest two possibilities (with the previously described caveat). First, BMECs preferentially oxidize the glucose and consequently there is no change in the amount that is shunted through glycolysis. Alternatively, BMECs need such low amount of glucose to meet their bioenergetics demands that increasing the concentration extracellularly has no effect on the amount taken up and utilized by the BMECs, and as such, they utilize equal amounts of glucose in control (25 mM glucose) medium and hyperglycemia (125 mM) NB.

We investigated whether the addition of the HKII inhibitor 3-BP[58] affected the rate of or amount of glucose consumed and lactate produced. HKII is a key enzyme in glycolysis that immediately converts glucose to glucose-6-phosphate (G6P)[59] when glucose is transported into the cell. Importantly, glycolysis cannot proceed if glucose is not first converted to G6P. While we previously have shown that the addition of 3-BP causes TEER to drop slightly for 24 hours, there was no effect on glucose consumption of lactate production compared to control cells. In addition to its role in glycolysis, HKII is closely associated with the mitochondria and known to also regulate the mitochondrial voltage dependent anion channel 1 (VDAC1)[60]. Thus, while inhibiting HKII does not appear to have any effect on glycolysis based on the fact that there is no change in lactate production, we can speculate that its effect on TEER arises from altering the interaction with mitochondria and VDAC1, though many more experiments are required to support this.

In addition to studying how BMECs utilize glucose, we assessed live cell metabolic status using the Seahorse XFe96 assay. We cultured BMECs in NB medium or DMEM and measured the response to compounds that inhibit different steps of mitochondrial metabolism. Although BMECs cultured in DMEM have significantly lower TEER than BMECs in NB medium, the Seahorse data suggests that BMECs in DMEM have a higher baseline OCR and rate of ATP production than BMECs in NB medium. Additionally, as described in section 4.2b, this assay begins by measuring baseline metabolic status, and eventually injects FCCP to force the cells to reach their maximum respiration. Interestingly, the data suggests that BMECs are functioning at their maximum respiratory capability while under the baseline conditions when cultured in both DMEM and NB medium. Taken together with the YSI data, there are a few possible explanations. Since the YSI data suggests that BMECs use very low amounts of glucose and produce low levels of lactate, one possibility is that BMECs are strongly utilizing ox-phos to meet their bioenergetics demands. Since the baseline OCR is approximately equal to maximum levels, it is feasible that BMECs oxidize a majority of the glucose, amino acids, and other nutrients to meet their demands under basal conditions, and as such, inducing maximum respiration results in no difference.

Finally, we sought to visualize mitochondria structure in BMECs under different media conditions. Mitochondria dynamics can have significant effects on cellular metabolism. In fact, iPSCs have highly fragmented mitochondria, and are hyperglycolytic[62]. Accordingly, we imaged iPSC-derived BMECs in DMEM, NB medium, NB medium with 3-BP, and NB medium without amino acids using structured illumination microscopy, to determine if there were changes in mitochondrial phenotype that may indicate metabolic differences. However, the BMECs seem to retain their long, elaborate networks under each of these conditions. Collectively, our data points to BMECs utilizing ox-phos to meet their bioenergetics demands, yet they are metabolically flexible to survive in amino acid free, glucose free, and other metabolically stressful environments.

Chapter 5: Conclusions, Discussion, and Future Directions

The BBB is a highly specialized vascular system that strictly regulates the flow of substances into and out of the CNS. An intact BBB and properly functioning BBB is essential for maintaining neuronal health and preventing neurological disorders. It has become increasingly accepted that BBB dysfunction plays a role in nearly every neurodegenerative disease, including AD and PD. As such, gaining a complete understanding of the BBB and its components, specifically the BMECs, represents the possible identification of novel drug targets to treat neurodegenerative diseases, and could also lead to improved efficacy for drugs crossing the BBB to treat neurological symptoms. This work aimed to address both of these issues. First, we sought to develop a fully defined, simplified differentiation protocol for producing BMECs from human iPSCs. This is a significant improvement to previous BBB models in that it removed the influence of serum from the media, increasing differentiation consistency and providing a new platform for potential mechanistic studies, as well as an upgraded model to for drug screens, both targeting the BBB itself and to screen drugs/compounds that can cross the BBB.

We recognized BMEC metabolic regulation as an understudied component that may underlie some of the key features unique to BMECs such as their high-fidelity tight junctions and ATP-driven efflux transporters. Additionally, our fully defined differentiation schematic provided us with a valuable tool to investigate BBB metabolism and we adapted the model to utilize NB medium or DMEM in place of hESFM in order to have complete control of each compound in the system. Using DMEM and NB medium gave us the ability to manipulate the culture system in a unique way that was not possible in hESFM. Specifically, we could completely customize the media with the knowledge that any change we made to the media could be accounted for if there were differences in results. However, at the beginning of the work we noticed that differentiating and culturing in DMEM produced BMECs with significantly lower TEER than BMECs in NB medium. Moreover, this effect proved to be reversible, and BMECs were responsive to media changes at any point after they were subcultured. This large TEER differential was slightly surprising because DMEM and NB media are relatively similar. However, one major difference was in amino acid concentrations. Our own previous data suggested that amino acid metabolism was a key component to increased barrier function.

As such, we hypothesized that BMECs differed from peripheral ECs, utilizing amino acids and ox-phos rather than glycolysis to meet their bioenergetics demands. Remarkably, we showed that iPSC-derived BMECs could not only survive, but also maintain a high barrier function in the absence of all amino acids or glucose. However, we did not investigate the effect of removing both glucose and all of the amino acids. Our YSI data suggests that iPSC-derived BMECs shift to a different metabolic state in the absence of amino acids, but further work is needed to characterize how BMECs utilize glucose under amino acid deprivation. Likewise, iPSC-derived BMECs in hyperglycemic NB medium do not upregulate the rate of glycolysis, as indicated by no change in the amount of lactate produced compared to both normoglycemic (25 mM) media and euglycemic (5 mM) media. Despite the limitations of the hyperglycemic YSI experiments (discussed in section 4.3a and 4.4), our data suggests one of two possibilities. First, the data suggests that even in hyperglycemic media, iPSC-derived BMECs do not increase their uptake and utilization of glucose relative to control NB medium. Alternatively, iPSC-derived BMECs do in fact uptake more glucose, but instead of upregulating the rate of glycolysis, the glucose-derived pyruvate is shuttled to the mitochondria to be oxidized.

The cell mito-stress test is an assay using the Seahorse XFe96 technology to investigate how cells respond metabolically to mitochondrial stressors. This assay complements the YSI experiments because it provides us with the cell's ATP production from mitochondrial respiration and also informs us as to how the BMECs respond when put under oxidative metabolic stress, while the YSI is mostly characterizes a cell's preference towards glycolysis. Our Seahorse data shows that BMECs cultured in DMEM have a higher baseline and maximum OCR and ATP production rates compared to BMECs cultured in NB medium. Additionally, the data demonstrated that in both media, BMECs are functioning at maximum respiratory capacity while they are under basal, baseline conditions. Collectively, the YSI experiments and Seahorse data tend to suggest that BMECs are primarily utilizing ox-phos, with the metabolic flexibility to shunt some glucose towards glycolysis. Future work should utilize highly oxidative and more highly glycolytic cells to compare the BMECs to. Additionally, further experiments using radiolabeled glucose would inform the ratio of glucose shuttled towards glycolysis relative to glucose that eventually undergoes oxidative metabolism. Finally, metabolomics experiments could identify specific pathways utilized in BMECs under different media conditions and compared to peripheral ECs. This data would provide valuable details as to how BMECs respond to

altered environmental conditions. More importantly, we could potentially identify metabolic pathways unique to BMECs compared to peripheral ECs that could represent novel therapeutic targets and play critical role in our understanding of neurodegenerative diseases.

References

1. Obermeier, B., Daneman, R. & Ransohoff, R. M. Development, maintenance and disruption of the blood-brain barrier. *Nat Med* **19**, 1584–1596 (2013).
2. Ben-Zvi, A. *et al.* MSFD2A is critical for the formation and function of the blood brain barrier. *Nature* **509**, 507–511 (2014).
3. Andreone, B. J. *et al.* Blood-Brain Barrier Permeability Is Regulated by Lipid Transport-Dependent Suppression of Caveolae-Mediated Transcytosis. *Neuron* **94**, 581-594.e5 (2017).
4. Geier, E. G. *et al.* Profiling Solute Carrier Transporters in the Human Blood-Brain Barrier. *Clin Pharmacol Ther* **94**, 636–639 (2013).
5. Pardridge, W. M. Blood-brain barrier drug targeting: the future of brain drug development. *Mol. Interv.* **3**, 90–105, 51 (2003).
6. Daneman, R. The blood–brain barrier in health and disease. *Annals of Neurology* **72**, 648–672 (2012).
7. Ransohoff, R. M. & Engelhardt, B. The anatomical and cellular basis of immune surveillance in the central nervous system. *Nat. Rev. Immunol.* **12**, 623–635 (2012).
8. Cecchelli, R. *et al.* Modelling of the blood-brain barrier in drug discovery and development. *Nat Rev Drug Discov* **6**, 650–661 (2007).
9. Sivandzade, F. & Cucullo, L. In-vitro blood–brain barrier modeling: A review of modern and fast-advancing technologies. *J Cereb Blood Flow Metab* **38**, 1667–1681 (2018).
10. Winger, R. C., Koblinski, J. E., Kanda, T., Ransohoff, R. M. & Muller, W. A. Rapid Remodeling of Tight Junctions During Paracellular Diapedesis in a Human Model of the Blood-Brain Barrier. *J Immunol* **193**, 2427–2437 (2014).
11. Joó, F. & Karnushina, I. A procedure for the isolation of capillaries from rat brain. *Cytobios* **8**, 41–48 (1973).
12. Bowman, P. D., Ennis, S. R., Rarey, K. E., Betz, A. L. & Goldstein, G. W. Brain microvessel endothelial cells in tissue culture: a model for study of blood-brain barrier permeability. *Ann. Neurol.* **14**, 396–402 (1983).

13. Roux, F. & Couraud, P.-O. Rat brain endothelial cell lines for the study of blood-brain barrier permeability and transport functions. *Cell. Mol. Neurobiol.* **25**, 41–58 (2005).
14. Patabendige, A., Skinner, R. A. & Abbott, N. J. Establishment of a simplified in vitro porcine blood-brain barrier model with high transendothelial electrical resistance. *Brain Res.* **1521**, 1–15 (2013).
15. Roux, F. *et al.* Regulation of gamma-glutamyl transpeptidase and alkaline phosphatase activities in immortalized rat brain microvessel endothelial cells. *J. Cell. Physiol.* **159**, 101–113 (1994).
16. Regina, A. *et al.* Mrp1 multidrug resistance-associated protein and P-glycoprotein expression in rat brain microvessel endothelial cells. *J. Neurochem.* **71**, 705–715 (1998).
17. Weksler, B. B. *et al.* Blood-brain barrier-specific properties of a human adult brain endothelial cell line. *FASEB J.* **19**, 1872–1874 (2005).
18. Weksler, B., Romero, I. A. & Couraud, P.-O. The hCMEC/D3 cell line as a model of the human blood brain barrier. *Fluids Barriers CNS* **10**, 16 (2013).
19. Lippmann, E. S. *et al.* Derivation of blood-brain barrier endothelial cells from human pluripotent stem cells. *Nature Biotechnology* **30**, 783–791 (2012).
20. Lippmann, E. S., Al-Ahmad, A., Azarin, S. M., Palecek, S. P. & Shusta, E. V. A retinoic acid-enhanced, multicellular human blood-brain barrier model derived from stem cell sources. *Sci Rep* **4**, 4160 (2014).
21. Stebbins, M. J. *et al.* Activation of RARα, RARγ, or RXRα Increases Barrier Tightness in Human Induced Pluripotent Stem Cell-Derived Brain Endothelial Cells. *Biotechnol J* **13**, (2018).
22. Vatine, G. D. *et al.* Modeling Psychomotor Retardation using iPSCs from MCT8-Deficient Patients Indicates a Prominent Role for the Blood-Brain Barrier. *Cell Stem Cell* **20**, 831-843.e5 (2017).
23. Helms, H. C. *et al.* In vitro models of the blood-brain barrier: An overview of commonly used brain endothelial cell culture models and guidelines for their use. *J. Cereb. Blood Flow Metab.* **36**, 862–890 (2016).
24. Eelen, G. *et al.* Endothelial Cell Metabolism. *Physiological Reviews* **98**, 3–58 (2018).
25. De Bock, K. *et al.* Role of PFKFB3-Driven Glycolysis in Vessel Sprouting. *Cell* **154**, 651–663 (2013).
26. Krützfeldt, A., Spahr, R., Mertens, S., Siegmund, B. & Piper, H. M. Metabolism of exogenous substrates by coronary endothelial cells in culture. *J. Mol. Cell. Cardiol.* **22**, 1393–1404 (1990).

27. Metallo, C.M., Walther, J.L., & Stephanopoulos, G. Evaluation of 13C isotopic tracers for metabolixc flux analysis in mammalian cells. *J Biotechnol* **144,** 167-174 (2009).
28. Mookerjee, S.A., *et al*. Quantifying intracellular rates of glycolysis and oxidative ATP production and consumption using extracellular flux measurements. *J Biol Chem* **292**, 7189-7209 (2017).
29. Pfeiffer, T., Schuster, S., & Bonhoeffer, S. Cooperation and competition in the evolution of ATP-producing pathways. *Science* **292,** 504-507 (2001).
30. Liberti, M. V. & Locasale, J. W. The Warburg Effect: How Does it Benefit Cancer Cells? *Trends Biochem Sci* **41**, 211–218 (2016).
31. Warburg, O. The metabolism of carcinoma cells. *Cancer Research* **9**, (1925).
32. Warburg, O., Wind, F. & Negelein, E. THE METABOLISM OF TUMORS IN THE BODY. *J. Gen. Physiol.* **8**, 519–530 (1927).
33. Hunt, T. K. *et al.* Aerobically derived lactate stimulates revascularization and tissue repair via redox mechanisms. *Antioxid. Redox Signal.* **9**, 1115–1124 (2007).
34. Ruan, G.-X. & Kazlauskas, A. Lactate engages receptor tyrosine kinases Axl, Tie2, and vascular endothelial growth factor receptor 2 to activate phosphoinositide 3-kinase/Akt and promote angiogenesis. *J. Biol. Chem.* **288**, 21161–21172 (2013).
35. Kadlec, A.O *et al.* Mitochondrial signaling in the vascular endothelium: beyond reactive oxygen species. *Basic Res Cardiol* **111**, (2016).
36. Oldendorf, W. H. & Brown, W. J. Greater Number of Capillary Endothelial Cell Mitochondria in Brain Than in Muscle. *Experimental Biology and Medicine* **149**, 736–738 (1975).
37. Smith, Q. R. & Rapoport, S. I. Cerebrovascular permeability coefficients to sodium, potassium, and chloride. *J. Neurochem.* **46**, 1732–1742 (1986).
38. Appelt-Menzel, A. *et al.* Establishment of a Human Blood-Brain Barrier Co-culture Model Mimicking the Neurovascular Unit Using Induced Pluri- and Multipotent Stem Cells. *Stem Cell Reports* **8**, 894–906 (2017).
39. Hollmann, E. K. *et al.* Accelerated differentiation of human induced pluripotent stem cells to blood–brain barrier endothelial cells. *Fluids Barriers CNS* **14**, (2017).

40. Wilson, H. K., Canfield, S. G., Hjortness, M. K., Palecek, S. P. & Shusta, E. V. Exploring the effects of cell seeding density on the differentiation of human pluripotent stem cells to brain microvascular endothelial cells. *Fluids Barriers CNS* **12**, 13 (2015).
41. Chen, G. *et al.* Chemically defined conditions for human iPS cell derivation and culture. *Nat Methods* **8**, 424–429 (2011).
42. Lippmann, E. S., Estevez-Silva, M. C. & Ashton, R. S. Defined human pluripotent stem cell culture enables highly efficient neuroepithelium derivation without small molecule inhibitors. *Stem Cells* **32**, 1032–1042 (2014).
43. Schindelin, J. *et al.* Fiji: an open-source platform for biological-image analysis. *Nat. Methods* **9**, 676–682 (2012).
44. Kumar, K. K. *et al.* Cellular manganese content is developmentally regulated in human dopaminergic neurons. *Sci Rep* **4**, (2014).
45. Tidball, A. M. *et al.* Genomic Instability Associated with p53 Knockdown in the Generation of Huntington's Disease Human Induced Pluripotent Stem Cells. *PLoS ONE* **11**, e0150372 (2016).
46. Bottenstein, J.. (1985). Cell Culture in the Neurosciences (Boston, MA: Springer US)
47. Salvador, E., Shityakov, S. & Förster, C. Glucocorticoids and endothelial cell barrier function. *Cell Tissue Res.* **355**, 597–605 (2014).
48. Mantle, J. L., Min, L. & Lee, K. H. Minimum Transendothelial Electrical Resistance Thresholds for the Study of Small and Large Molecule Drug Transport in a Human in Vitro Blood-Brain Barrier Model. *Mol. Pharm.* **13**, 4191–4198 (2016).
49. Mantle, J. L., Min, L. & Lee, K. H. Minimum Transendothelial Electrical Resistance Thresholds for the Study of Small and Large Molecule Drug Transport in a Human in Vitro Blood-Brain Barrier Model. *Mol. Pharm.* **13**, 4191–4198 (2016).
50. Cheng, S. *et al.* Distinct Metabolomic Signatures Are Associated with Longevity in Humans. *Nat Commun* **6**, 6791 (2015).
51. Shah, S. H. *et al.* Baseline metabolomic profiles predict cardiovascular events in patients at risk for coronary artery disease. *Am. Heart J.* **163**, 844-850.e1 (2012).

52. Wang, T. J. *et al.* Metabolite Profiles and the Risk of Developing Diabetes. *Nat Med* **17**, 448–453 (2011).

53. Mathieu, P., Pibarot, P. & Després, J.-P. Metabolic Syndrome: The Danger Signal in Atherosclerosis. *Vasc Health Risk Manag* **2**, 285–302 (2006).

54. Tynkkynen, J. *et al.* Association of branched-chain amino acids and other circulating metabolites with risk of incident dementia and Alzheimer's disease: A prospective study in eight cohorts. *Alzheimers Dement* **14**, 723–733 (2018).

55. Varma, V. R. *et al.* Brain and blood metabolite signatures of pathology and progression in Alzheimer disease: A targeted metabolomics study. *PLoS Med.* **15**, e1002482 (2018).

56. Xiong, J. *et al.* A Metabolic Basis for Endothelial-to-Mesenchymal Transition. *Mol. Cell* **69**, 689-698.e7 (2018).

57. Neal, E. H. *et al.* A Simplified, Fully Defined Differentiation Scheme for Producing Blood-Brain Barrier Endothelial Cells from Human iPSCs. *Stem Cell Reports* **12**, 1380–1388 (2019).

58. Ganapathy-Kanniappan, S. *et al.* 3-bromopyruvate: a new targeted antiglycolytic agent and a promise for cancer therapy. *Curr Pharm Biotechnol* **11**, 510–517 (2010).

59. Patra, K. C. *et al.* Hexokinase 2 is required for tumor initiation and maintenance and its systemic deletion is therapeutic in mouse models of cancer. *Cancer Cell* **24**, 213–228 (2013).

60. Shoshan-Barmatz, V., Maldonado, E. N. & Krelin, Y. VDAC1 at the crossroads of cell metabolism, apoptosis and cell stress. *Cell Stress* **1**, 11–36 (2017).

61. Mannello, F. & Tonti, G. A. Concise review: no breakthroughs for human mesenchymal and embryonic stem cell culture: conditioned medium, feeder layer, or feeder-free; medium with fetal calf serum, human serum, or enriched plasma; serum-free, serum replacement nonconditioned medium, or ad hoc formula? All that glitters is not gold! *Stem Cells* **25**, 1603–1609 (2007).

62. Rasmussen, M. L. *et al.* A Non-apoptotic Function of MCL-1 in Promoting Pluripotency and Modulating Mitochondrial Dynamics in Stem Cells. *Stem Cell Reports* **10**, 684–692 (2018).

63. Chen, H. & Chan, D. C. Mitochondrial dynamics in regulating the unique phenotypes of cancer and stem cells. *Cell Metab* **26**, 39–48 (2017).